Heliyon 11 (2025) e41693

Contents lists available at ScienceDirect

Heliyon

journal homepage: www.cell.com/heliyon

Research article

Modelling climate change and aridity for climate impact studies in semi-arid regions: The case of Giba basin, northern Ethiopia

Atsbha Brhane Gebru [a,b,*], Tesfamichael Gebreyohannes [a], Gebrerufael Hailu Kahsay [c]

[a] School of Earth Sciences, Mekelle University, P.O. Box 231, Mekelle, Ethiopia
[b] School of Water Technology, Aksum University, P.O. Box 314, Shire-Campus, Shire, Ethiopia
[c] Institute of Geo-information and Earth Observation Sciences, Mekelle University, P.O. Box 231, Mekelle, Ethiopia

ARTICLE INFO

Keywords:
Climate variability
Giba basin
Projection
RCP
SDSM

ABSTRACT

Analysis: of long-term and future climate variability is crucial for impact assessment studies in drought-prone areas like the Giba basin in northern Ethiopia. This study has applied the statistical downscaling model (SDSM) and (De Martonne and Pinna combinative) aridity index methods to evaluate the climate system of the Giba basin. Historical data (1961–2019) from seven meteorological stations and global grided data were used for future climate projections (2020–2100) under the three emission scenarios (RCPs 2.6, 4.5, and 8.5) for the three-time horizons (2040s, 2060s, and 2080s). Analysis of results showed that rainfall and temperature projection on a monthly and/or seasonal basis has more significance than on an annual basis for impact studies particularly, in areas where irrigation practices are common like in the Giba basin. Seasonal projection of rainfall in the basin showed a slightly decreasing trend during the spring season (MAM), and a significant increment in the main rainy season (JJA) under all scenarios and for the whole projection year. On an annual basis, a maximum increase of rainfall, up to +285 mm/year and +298 mm/year was expected to increase at Abyi Adi and Mekelle Obs stations, respectively, under RCP 8.5 in the 2080s. Temperature projection showed a consistent rise throughout the basin that ranges from a minimum increase of Tmax by +0.29 °C in the 2040s (RCP 2.6) at Mekelle Obs station to a maximum increase of Tmin by +2.35 °C in the 2080s (RCP8.5) at Abyi Adi station. In general, it is observed that the rate of increment of projected Tmin was more than that of Tmax in all stations in the Giba basin, which showed a continuous contraction of the gap between Tmin and Tmax, hence, the prevalence of global warming. This has led to a considerable increment of aridity till the end of the 21st century. Hence, the implementation of locally-suited climate change resilient strategies is crucial to enhance the sustainability of the ecosystem and ensure food security in the basin.

1. Introduction

Climate projection studies for the 21st century show diverging trends of rainfall and temperature variability in different parts of Ethiopia. For instance, an increase in both rainfall and temperature during the middle and end of the century was reported in central

* Corresponding author. School of Earth Sciences, Mekelle University, P.O. Box 231, Mekelle, Ethiopia.
E-mail address: atsbha.brhane@gmail.com (A.B. Gebru).

https://doi.org/10.1016/j.heliyon.2025.e41693
Received 2 August 2024; Received in revised form 20 December 2024; Accepted 2 January 2025
Available online 4 January 2025

[1–3], northwestern [4], and northern Ethiopia [5,6]. Similarly, projections of increased mean annual temperature and decreased rainfall during the wet months (June, July, August, and September) were reported in southwest [7], western [8], and northeastern Ethiopia [9].

The increase in climate variability in the 21st century is expected to hamper agricultural productivity [10] and exacerbate the vulnerability of water resources to climate change in East Africa [11]. Hence, understanding rainfall and temperature variability is crucial for sustainable development and management of water resources [12–14] and enhancing resilience to droughts [15,16] through the formulation of mitigation and adaptation measures that stem from climate projections of high spatial and temporal resolution [17].

General circulation models (GCMs) are currently used to understand and analyze large-scale variations of climate variables globally [18]. However, the coarse spatial resolution (>100 km) of GCMs [17,19] and associated uncertainties and biases [20] limit their applicability for impact assessment studies at a local scale. These limitations can be decreased through downscaling mechanisms, i.e., by narrowing the gap between the coarser scale of GCMs and finer resolution (impact models) required for intended purposes [21–24]. In this regard, the statistical downscaling model (SDSM) and dynamical downscaling techniques are commonly used methods for the generation of high-resolution climate scenarios [25]. Comparing these two methods, the SDSM is better than a dynamical downscaling model for generating station data that is important for impact assessment studies [26] and also enables for identification of sources of uncertainties in climate models [27]. Moreover, the use of climate indices, which are diagnostic tools for the analysis of climate change [28,29] is crucial to better understand the state of the climate system [30].

The Giba basin is one of the most densely populated and urbanized parts of northern Ethiopia where the capital city of Tigray, Mekelle, and other urban areas such as Abyi Adi, Hagereselam, Wukro, Fireweyni, Edaga Hamus and Hawzen are located. The basin is a hub for millions of populations that are solely dependent on rainfed agriculture, and to some extent on irrigation [31–33]. The Aynalem wellfield, which is one of the most important wellfields in Ethiopia [34] and that has been providing domestic and industrial water supply to Mekelle city for the last three decades is also located in this basin. Thus, the Giba basin has significant importance for socioeconomic development [35]. Previous research studies show that the Giba basin is a water-stressed area with only a short rainy

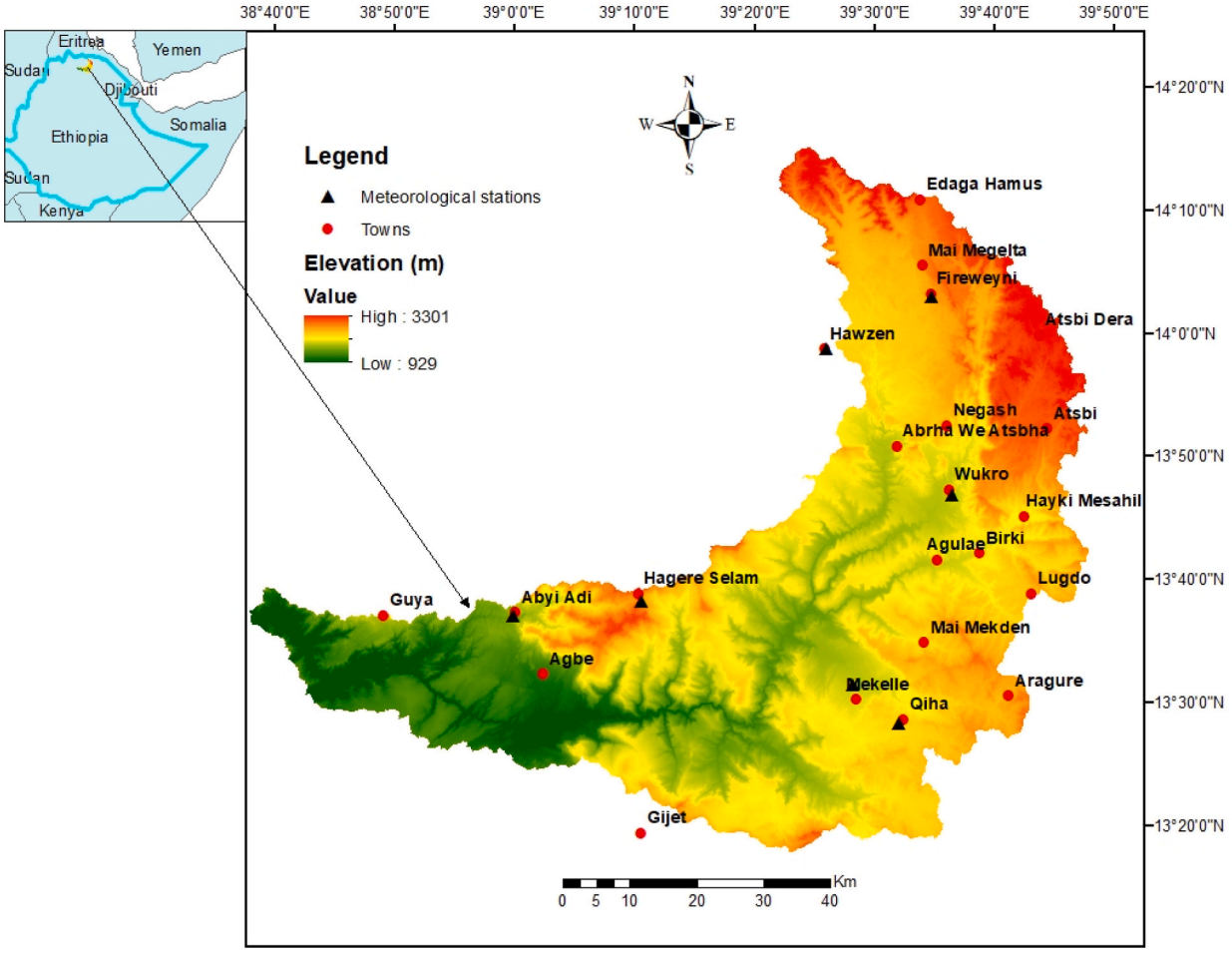

Fig. 1. Geographical location of the study area.

period from June to August, and consequently crop water deficit to be supplemented by groundwater abstraction during the dry season is increasing [32,36–38]. This is in line with the FAO projection that global agricultural water abstraction by 2030 will be about 14 % higher than the abstraction in 2000 due to population growth and climate change [39]. Similarly, research experiences at a global scale suggest that climate change affects every component of the ecosystem including water quantity and quality [40], soil nutrient quality [41], crop production [42], livestock husbandry [43], and vegetation. This, in turn, affects the whole food systems [44] and consequently, increases the prevalence of malnourishment rate and food insecurity particularly in the Sub-Saharan region [44,45]. Therefore, a detailed understanding of future climate variability in specific local conditions is crucial to adequately respond to the impact of climate change on the various sectors [46]. However, the long-term future climate variability remains uncertain and not adequately known in the Giba basin. Hence, assessment and evaluation of long-term projected climatic variability under the IPCC Representative Concentration Pathways (RCPs) is crucial to propose and implement appropriate climate adaptation and mitigation strategies at a local scale in the basin. To this end, this study attempted (i) to analyze historical and future climate (particularly rainfall, maximum and minimum temperature) variability, and (ii) to evaluate the aridity of the climate system of the Giba basin. This study is unique in terms of integrating climate change and aridity indices to project future scenarios under the three RCPs in the Giba basin. The findings of this study will be useful input for climate impact assessment studies that make use of projected temperature and rainfall data and preparation of climate-change resilient strategies for the basin in particular and semi-arid regions in general.

2. Methodology

2.1. Study area

The Giba basin (5260 km^2 surface area) is located in Tigray regional state, northern Ethiopia, between longitudes of 38°40′ and 39°50′ east and latitudes of 13°20′ and 14°20’ north (Fig. 1). The basin is drained by the Giba River, that flows to the Tekeze River, which joins the Blue Nile River in Sudan. The basin is characterized by rugged topography where elevation ranges from 929 to 3300 m (Fig. 1), and undulating metamorphic terrain, deep gorges Mesozoic sedimentary terrain, and steep volcanic mountains dominate in the southwestern and northeastern, central, and northern and southwest of the central parts of the basin, respectively [37].

The rainfall pattern of the basin is characterized by a bimodal, rainy season (mid-June till mid-September) and the spring season (mid-March till mid-June) that constitute 11–25 % and 69–85 % of the mean annual rainfall, respectively. The climate of the basin is semi-arid, with a mean annual rainfall ranging from 550 mm in the eastern and northern parts to 600 mm in the middle part, and 1050 mm in the western parts (from the data taken from the seven meteorological stations used in the current study). Long-term average maximum temperature ranges from 22.3 to 24.1 °C in the highland areas and 27.4–29.8 °C in the low-lying areas. Similarly, the long-term average minimum temperature varies from 10.3 to 11.1 °C and 11.3–13.7 °C in the highland and lowland areas, respectively (Table 1). Annual average potential evapotranspiration (PET) in the basin is 1693 mm [47]. Livelihood in the basin is solely reliant on rainfed agriculture and to some extent on irrigation during the dry season.

2.2. Datasets

Observed climate data (also called predictands) including observed daily precipitation, and maximum and minimum temperature (Tmax and Tmin) for the years 1961–2019 were collected from the National Meteorological Agency of Ethiopia - Mekelle branch (Table 1).

The seven meteorological stations have full meteorological records of the principal climate variables except the three-year missed data in the 1980s because of the total rain failure and instability in the region [48,46]. These missed data were filled by using ready-to-use freely available weather data from the Climate Forecast System Reanalysis (CFSR, availabl1e at: http://globalweather.tamu.edu). The CFSR is a global atmospheric dataset with a spatial resolution of approximately 38 km [49]. They are useful, particularly in data-limited developing countries like Ethiopia, and are accurate as they combine ground-based observational data and bias-corrected satellite data [50].

Analysis of long-term average monthly temperature and rainfall shows that Abyi Adi station has the highest records of both rainfall

Table 1
Description of data availability at the seven stations in the Giba basin.

Station name	Location (UTM)			Number of record years	Mean annual rainfall (mm)	Mean annual Tmax (°C)	Mean annual Tmin (°C)
	Longitude	Latitude	Elevation (m.a.s.l)				
Abyi Adi	38°59′55″	13°37′16″	1846	22	1084	29.8	13.7
Hagereselam	39°10′14″	13°39′5″	2636	26	707	22.3	11.1
Hawzen	39°26′14″	13°58′56″	2265	28	543	27.3	10.3
Mekelle Airport (AP)	39°32′6″	13°28′8″	2252	60	600	24.5	11.3
Mekelle Observatory (Obs)	39°28′2″	13°31′30″	1994	17	559	27.4	12.2
Fireweyni	39°34′39″	14°03′4″	2486	19	553	24.1	11.1
Wukro	39°36′22″	13°46′55″	2003	28	603	27.9	11.3

and temperature as compared to the other six stations in the Giba basin (Fig. 2).

Mean annual rainfall at Abyi Adi station is about 1084 mm and mean monthly temperature ranges from 20.4 °C in December to 23.8 °C in May. Contrary to this, Hagereselam station has records of relatively low temperatures, and Hawzen, Fireweyni, and Mekelle Obs stations have the lowest records of rainfall.

Considering the long-term monthly average temperature of the basin, May and December are the hottest and coldest months at all meteorological stations, respectively. Identification of the hottest and coldest months, and analysis of monthly and/or seasonal rainfall is crucial for irrigation scheduling in areas where irrigation practices are common like the Giba basin. Long-term historical rainfall and temperature variability in the majority of meteorological stations in the Giba basin has shown increasing and/or decreasing trends (Fig. 3). For instance, long-term annual rainfall showed a slightly decreasing trend at Mekelle AP and Fireweyni stations, and a slightly increasing trend at Hawzen, Mekelle Obs, and Wukro stations. Rainfall did not show a noticeable trend at Abyi Adi and Hagereselam stations. Similarly, the mean annual temperature showed an increasing trend in the majority of the stations, e.g., at Abyi Adi, Hagereselam, Hawzen, Mekelle Obs, and Wukro stations. A decrease in temperature was observed at Fireweyni station, and almost no trend of visible temperature change occurred at Mekelle AP station. Generally, it is noticeable that the magnitude of the change of temperature is more pronounced than that of rainfall throughout the Giba basin during the last decades.

Predictor variables (Table 2) were derived from the reanalysis data of the Canadian National Centers for Environmental Prediction (NCEP) [51] for the SDSM calibration (1961–1990) and validation (1991–2005). Predictor data from the second-generation Canadian Earth System Model (CanESM2) were used for future climate projections (2020–2100) under three Representative Concentration Pathways (RCPs), namely, RCP2.6, RCP4.5, and RCP8.5 (available at http://climate-scenarios.canada.ca/). The predictor variables are available at a spatial resolution of nearly uniform latitude and longitude of about 2.8125°.

2.3. Methods

The SDSM is a widely used model for downscaling future climate projections [21] by using the 26 GCM predictors (Table 2). It employs a multi-linear regression method by using a statistical relationship between the predictands and predictors. The model enables to perform multiple tasks such as data quality control, predictor screening, model calibration and validation, and generation of climate scenarios. Appropriate selection of the predictors defines the accuracy of the model [46], and one of the most challenging tasks in applying the SDSM is screening predictors, particularly for precipitation. Predictor selection was made by displaying scatterplots, and making an analysis of the statistical significance ($P < 0.05$) of predictor-predictand relationships, and through correlation and partial correlation (r) analysis.

The model produces up to 100 daily weather ensembles (which are considered to be equally reasonable) by taking a single predictand (e.g., daily precipitation) and selected NCEP predictors (e.g., ncepprcpgl, nceps500gl, ncepshumgl, and ncepp5_ugl). Accordingly, predictor variables with the highest p-value and lowest r-value were selected as these values determine highest sensitivity of the variables. Following this screening step, model calibration and validation, and future projection steps were carried out using the NCEP and CanESM2 ensembles, respectively. Finally, the output result was compared with the station data by using statistical parameters. Fig. 4 represents the methodology.

As per the recommendation by Moriasi et al. [53], root mean square error (RMSE), coefficient of determination (R^2), percent bias (Pbias), and Nash–Sutcliffe coefficient (NSE) are the most commonly used techniques to evaluate the performance of models. Accordingly, these four statistical approaches were applied in this study to examine the performance of the SDSM (Eqs. (1)–(4)). The RMSE values show the level of fitness between observed and simulated data, in which lower values indicate the high accuracy of the model. The R^2 (values range from 0 to 1) indicates the relationship between simulated and observed data, whereas the Pbias shows the average tendency of simulated data to be bigger or smaller than the observed data. According to this technique, a zero value indicates a highly accurate model, while negative and positive values indicate overestimation and underestimation of the model respectively. The NSE [54] is used for determining the relative magnitude of the residual variance by comparing it to the observed variance [55].

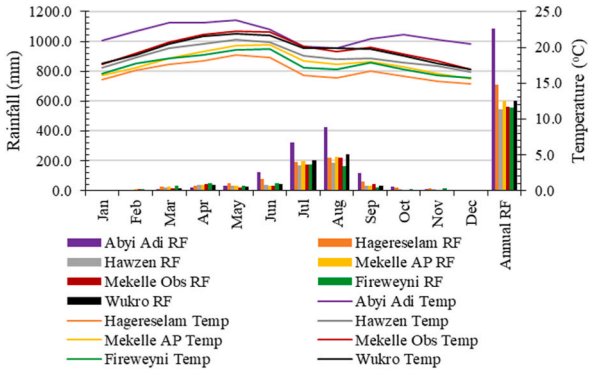

Fig. 2. Average monthly temperature (°C) and monthly and annual rainfall (mm) for the seven meteorological stations in the study period (1961–2019).

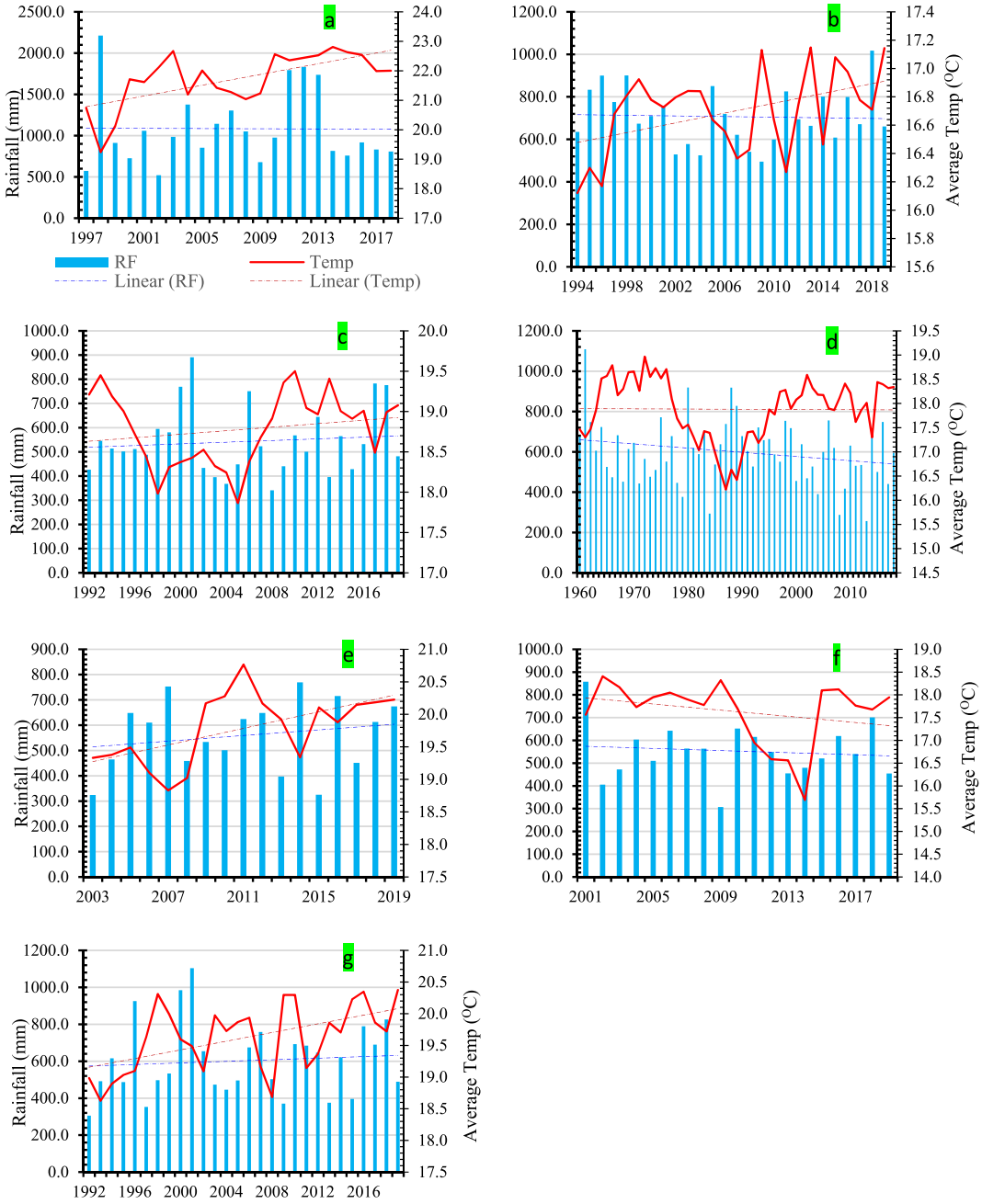

Fig. 3. Long-term historical trends of rainfall and temperature in Abyi Adi (a), Hagereselam (b), Hawzen (c), Mekelle AP (d), Mekelle Obs (e), Fireweyni (f), and Wukro (g) stations in the Giba basin.

$$RMSE = \sqrt{\frac{\sum_{i=1}^{n} (x_s - x_o)^2}{n}} \tag{1}$$

$$R^2 = \frac{\sum_{n=1}^{n} (x_o - \bar{x}_o)(x_s - \bar{x}_s)}{\sqrt{\sum_{i=1}^{n} (x_o - \bar{x}_o)^2 \sum_{i=1}^{n} (x_s - \bar{x}_s)^2}} \tag{2}$$

Table 2
List of NCEP predictor variables used for calibration and validation of SDSM [52].

No	Code	Description	No	Code	Description
1	ncepmslpgl	Mean sea level pressure	14	ncepp5zhgl	500 hPa divergence
2	ncepp1_fgl	Surface airflow strength	15	ncepp8_fgl	850 hPa airflow strength
3	ncepp1_ugl	Surface zonal velocity	16	ncepp8_ugl	850 hPa zonal velocity
4	ncepp1_vgl	Surface meridional velocity	17	ncepp8_vgl	850 hPa meridional velocity
5	ncepp1_zgl	Surface vorticity	18	ncepp8_zgl	850 hPa vorticity
6	ncepp1thgl	Surface wind direction	19	ncepp850gl	850 hPa geopotential height
7	ncepp1zhgl	Surface divergence	20	ncepp8thgl	850 hPa wind direction
8	ncepp5_fgl	500 hPa airflow strength	21	ncepp8zhgl	850 hPa divergence
9	ncepp5_ugl	500 hPa zonal velocity	22	ncepprcpgl	Precipitation
10	ncepp5_vgl	500 hPa meridional velocity	23	nceps500gl	Specific humidity at 500 hPa
11	ncepp5_zgl	500 hPa vorticity	24	nceps850gl	Specific humidity at 850 hPa
12	ncepp500gl	500 hPa geopotential height	25	ncepshumgl	Surface specific humidity
13	ncepp5thgl	500 hPa wind direction	26	nceptempgl	Mean temperature at 2 m

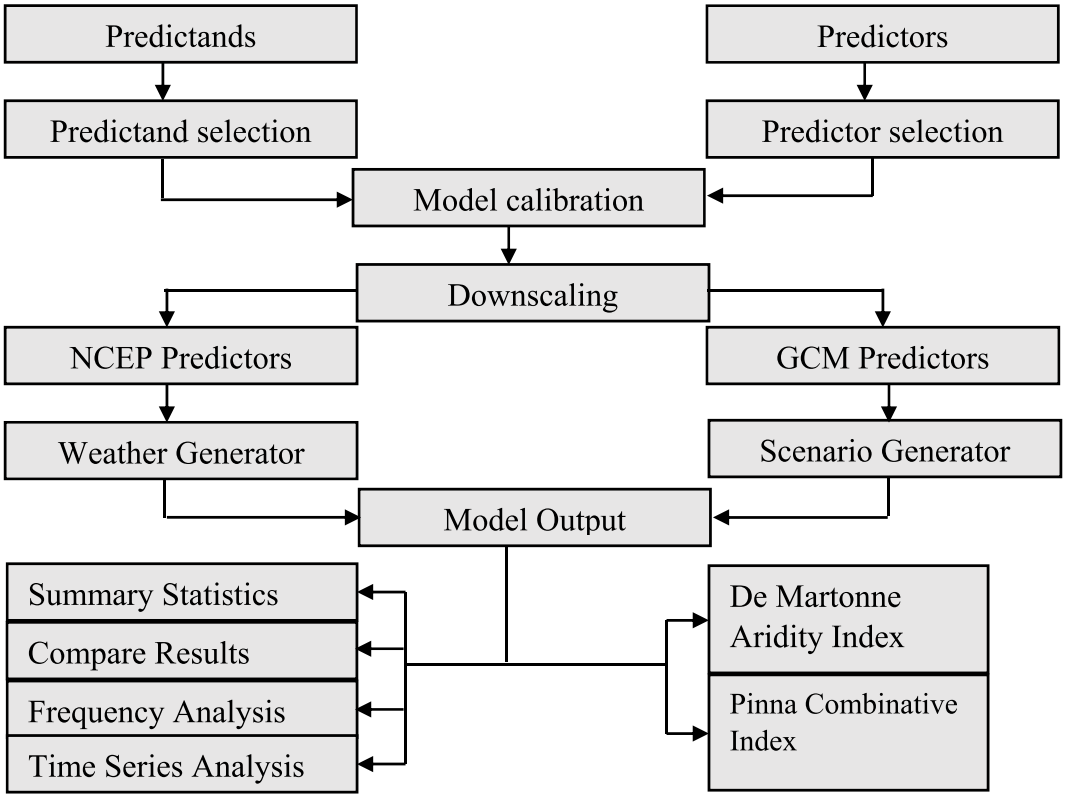

Fig. 4. SDSM process and climate indices.

$$\text{Pbias} = \frac{\sum_{i=1}^{n}(x_s - x_o)}{\sum_{i=1}^{n}(x_o)} * 100 \tag{3}$$

$$\text{NSE} = 1 - \frac{\sum_{i=1}^{n}(x_o - x_s)^2}{\sum_{i=1}^{n}(x_o - \overline{x}_s)^2} \tag{4}$$

Where x_o denotes the observed data, $\overline{x}_o$ the average observed data, x_s the simulated data, $\overline{x}_s$ the average simulated data, and n denotes the number of measured data points.

In this study, two climate indices, namely, the De Martonne aridity index and Pinna combinative index, which are frequently used

globally [56] and considered aridity-humidity indices [28,53] were used to classify the historical and future climatic conditions of the area. Aridity indicates moisture deficiency which results from the absence of sufficient rainfall and at the same time high evapotranspiration rates. The De Martonne aridity index can be computed on a monthly, seasonal, and annual basis to classify the climatic condition based on the duration of the aridity [51,54]. The De Martonne aridity index values on annual and monthly basis were calculated using Eq. (5) and Eq. (6), respectively.

$$I_{DM} = \frac{P}{T + 10} \tag{5}$$

Where I_{DM} is the De Martonne aridity index, P is the mean annual precipitation in mm, and T is the mean annual temperature in degrees Celsius. Table 3 presents the climate classification based on the I_{DM} values.

$$I_M = \frac{12\overline{P}}{\overline{T} + 10} \tag{6}$$

Quantification of the De Martonne aridity index on a monthly basis (Eq. (6)) is important for decision-making on different activities such as the need to irrigate the land in that month [57]. Hence, the De Martonne aridity index for the baseline and future periods (under the three scenarios) was computed on a monthly basis, and the percentage change was computed using Eq. (7).

$$\%I_M = \left(\frac{F_{IM} - B_{IM}}{B_{IM}}\right) \tag{7}$$

Where, $\%I_M$ is the % change of De Martonne monthly index value, and F_{IM} and B_{IM} are the monthly future and baseline De Martonne index values, respectively.

Similar to the De Martonne aridity index, Pinna combinative index (Eq. (8)) values less than 10, and between 10 and 20 represent arid and semiarid climatic conditions, respectively. The Pinna combinative index takes precipitation and temperature of the driest month into account, which in turn makes it more helpful in identifying the seasons where irrigation is needed [28].

$$I_P = \frac{1}{2}\left(\frac{P}{T + 10} + \frac{12\overline{P}_d}{\overline{T}_d + 10}\right) \tag{8}$$

Where I_P is the Pinna combinative index, P and T are mean annual precipitation and temperature, and P_d and T_d are precipitation and temperature averages in the driest month, respectively.

3. Results and discussion

3.1. Screening of predictors and performance assessment of SDSM

Table 4 summarizes the most influential predictors for downscaling rainfall, Tmax, and Tmin variables at all stations in the Giba basin. The types of predictors for rainfall and temperature variables vary among the stations throughout the basin.

The nceptempgl is the most influencing predictor (highest partial correlation, r) for Tmax and Tmin in all stations. Other predictors such as ncepp8_vgl and ncepp5thgl (for Tmax), and ncepp1_ugl and ncepshumgl are also influential in the majority of the stations. The influence of temperature predictor variables looks in alignment with elevation differences. In other words, the same predictors such as ncepshumgl and ncepp8_vgl for Tmin and Tmax, respectively, are influential in elevated areas such as Hagereselam, Hawzen, and Fireweyni stations.

The driving factors for rainfall varied among the stations except the ncepshumgl which is common in Hagereselam, Hawzen, and Mekelle Obs stations (Table 4). This also indicates screening of predictor variables for rainfall is difficult compared to temperature.

The performance of SDSM was evaluated using statistical evaluation methods for the calibration and validation periods (Table 5). The calibration and validation results show that there was a strong statistical agreement between observed and modeled rainfall, Tmax, and Tmin variables. Fig. 6 shows a comparison of observed and modeled rainfall and temperature variables during the calibration and validation periods for the Mekelle AP station. The downscaling process produced almost a perfect fit of synthetic temperature data and showed an excellent performance in generating rainfall data for all stations in the Giba basin (Fig. 5 and Table 5).

Table 3
De Martonne climate index classification.

Climate	I_{DM} values	Precipitation, P values (mm)
Dry	$I_{DM} < 10$	$P < 200$
Semi-dry	$10 \leq I_{DM} < 20$	$200 \leq P < 400$
Mediterranean	$20 \leq$ IDM <24	$400 \leq P < 500$
Semi-humid	$24 \leq$ IDM <28	$500 \leq P < 600$
Humid	$28 \leq$ IDM <35	$600 \leq P < 700$
Very humid	IDM ≥ 35	$P \geq 700$

Table 4
Climate variables with their respective selected NCEP predictors per station.

Station	Climate variables	NCEP Predictors	Partial r	P-value
Hagere Selam	Tmax	ncepp5thgl	0.163	0.0000
		ncepp8_vgl	0.079	0.0000
		nceptempgl	0.482	0.0000
	Tmin	ncepp1_ugl	0.245	0.0000
		ncepshumgl	0.209	0.0000
		nceptempgl	0.522	0.0000
	RF	ncepp1zhgl	0.048	0.0528
		ncepshumgl	0.020	0.3769
Abyi Adi	Tmax	ncepp5thgl	0.150	0.0000
		ncepp8_vgl	0.139	0.0000
		nceptempgl	0.431	0.0000
	Tmin	ncepp500gl	0.204	0.0000
		nceptempgl	0.160	0.0000
	RF	ncepp8_ugl	0.029	0.2731
		ncepp850gl	0.105	0.0000
Wukro	Tmax	ncepp1_zgl	0.061	0.0000
		nceptempgl	0.361	0.0000
	Tmin	ncepp1_ugl	0.165	0.0000
		ncepp500gl	0.111	0.0000
		nceptempgl	0.329	0.0000
	RF	ncepmslpgl	0.041	0.1689
		ncepp8_ugl	0.046	0.1259
Fireweyni	Tmax	ncepp5thgl	0.162	0.0000
		ncepp8_zgl	0.137	0.0000
		nceptempgl	0.221	0.0000
	Tmin	ncepprcpgl	0.100	0.0000
		ncepshumgl	0.202	0.0000
		nceptempgl	0.346	0.0000
	RF	ncepp5_fgl	0.050	0.1420
		ncepprcpgl	0.039	0.2419
Hawzen	Tmax	ncepp5_ugl	0.195	0.0000
		ncepp8_vgl	0.188	0.0000
		nceptempgl	0.329	0.0000
	Tmin	ncepp1zhgl	0.213	0.0000
		ncepshumgl	0.249	0.0000
		nceptempgl	0.478	0.0000
	RF	ncepp1_fgl	0.072	0.0064
		ncepp5zhgl	0.047	0.0826
		ncepshumgl	0.054	0.0477
Mekelle AP	Tmax	nceptempgl	0.074	0.0000
		ncepshumgl	0.459	0.0000
	Tmin	ncepp1_ugl	0.101	0.0000
		ncepprcpgl	0.119	0.0000
		nceptempgl	0.487	0.0000
	RF	ncepp1_zgl	0.051	0.0089
		nceps500gl	0.103	0.0000
Mekelle Obs	Tmax	ncepp8_vgl	0.067	0.0000
		nceps850gl	0.057	0.0001
		nceptempgl	0.490	0.0000
	Tmin	ncepp1_ugl	0.114	0.0000
		nceps500gl	0.099	0.0000
		nceptempgl	0.481	0.0000
	RF	ncepp1_vgl	0.028	0.3774
		ncepshumgl	0.065	0.0618

3.2. Prediction of future rainfall and temperature scenarios

3.2.1. Prediction of future rainfall

Change in Tmax and Tmin and rainfall is graphically presented for three stations (Abyi Adi, Wukro, and Hagereselam) to represent the highest - medium - lowest ranges of temperature and rainfall variables in the Giba basin respectively (Figs. 6–8). Rainfall and temperature projection (on annual basis) for 2040s, 2060s, and 2080s vary among stations in the Giba basin (Table 6). For instance, rainfall is expected to increase in all three scenarios in all stations in the Giba basin except the Fireweyni station. At Fireweyni station, annual rainfall is expected to slightly decrease by nearly −10 mm (RCP 2.6) and −5 mm (RCP 4.5) in the 2040s. However, it is expected to increase up to +44 mm/year during the 2080s for the RCP 8.5 scenario. The high amount of rainfall, i.e., up to +285 mm/year and +298 mm/year is expected to increase at the Abyi Adi and Mekelle Obs stations, respectively, for the RCP 8.5 scenario in the 2080s (Annex 1).

Table 5
Performance indicators of SDSM for the calibration and validation periods.

Station name	Climate variable	RMSE	R^2	Pbias	NSE
		Calibration (validation)	Calibration (validation)	Calibration (validation)	Calibration (validation)
Hagere Selam	Tmax	0.045 (0.051)	0.990 (0.995)	−0.001 (0.018)	0.999 (0.999)
	Tmin	0.006 (0.014)	0.999 (0.994)	0.002 (0.007)	0.999 (0.999)
	Rainfall	1.743 (3.710)	0.995 (0.939)	0.468 (1.030)	0.999 (0.997)
Abyi Adi	Tmax	0.043 (0.028)	0.998 (0.989)	0.003 (−0.009)	0.999 (0.999)
	Tmin	0.017 (0.033)	0.999 (0.998)	0.009 (−0.018)	0.999 (0.999)
	Rainfall	1.728 (1.836)	0.970 (0.981)	0.700 (−0.725)	0.999 (0.999)
Wukro	Tmax	0.013 (0.021)	0.987 (0.995)	−0.012 (0.001)	0.999 (0.999)
	Tmin	0.019 (0.024)	0.999 (0.999)	0.102 (0.044)	0.999 (0.999)
	Rainfall	2.730 (2.012)	0.999 (0.999)	−2.020 (−1.353)	0.999 (0.999)
Fireweyni	Tmax	0.215 (0.035)	0.949(0.999)	0.082 (0.005)	0.979 (0.999)
	Tmin	0.018 (0.010)	0.998 (0.999)	0.003 (0.007)	0.999 (0.999)
	Rainfall	2.545 (3.601)	0.934 (0.932)	0.364 (1.140)	0.998 (0.996)
Hawzen	Tmax	0.009 (0.009)	0.999 (0.994)	−0.002 (−0.003)	0.999 (0.999)
	Tmin	0.016 (0.006)	0.996 (0.998)	0.005 (−0.003)	0.999 (0.999)
	Rainfall	2.545 (1.946)	0.927 (0.955)	1.155 (0.382)	0.998 (0.998)
Mekelle AP	Tmax	0.035 (0.053)	0.999 (0.997)	0.011 (−0.007)	0.999 (0.998)
	Tmin	0.013 (0.015)	0.998 (0.995)	−0.003 (0.006)	0.999 (0.999)
	Rainfall	1.233 (1.507)	0.986 (0.990)	0.722 (−0.235)	0.999 (0.999)
Mekelle Obs	Tmax	0.016 (0.015)	0.999 (0.995)	0.001 (−0.007)	0.999 (0.999)
	Tmin	0.027 (0.041)	0.997 (0.987)	0.007 (0.016)	0.999 (0.999)
	Rainfall	1.751 (2.766)	0.983 (0.998)	0.013 (−1.225)	0.998 (0.966)

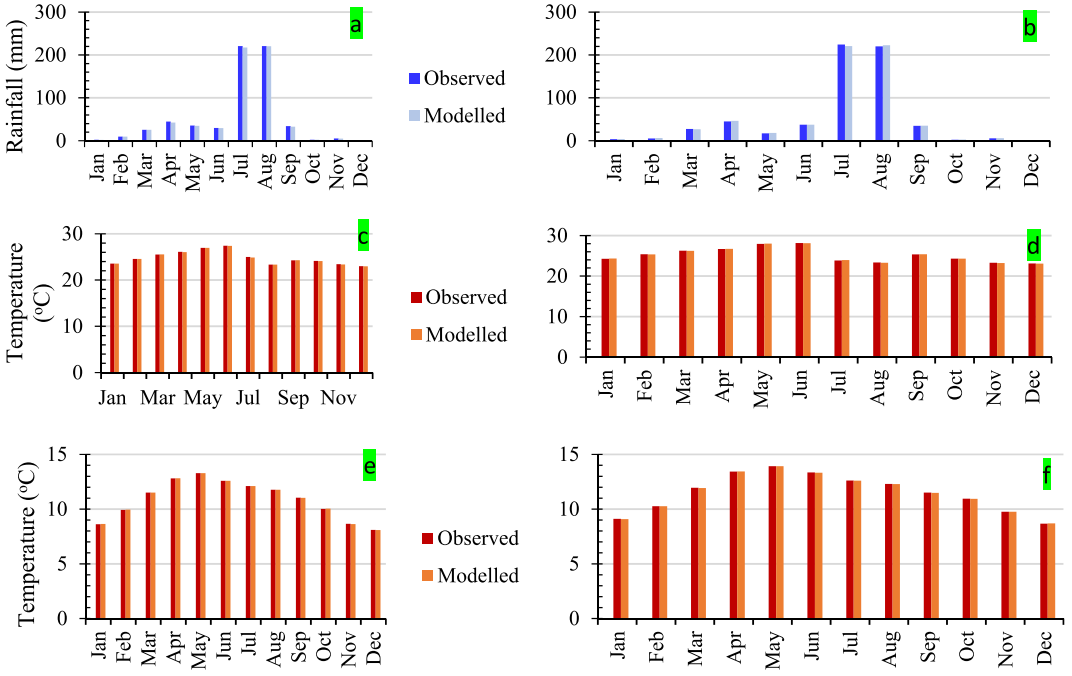

Fig. 5. Calibration of monthly rainfall (a), mean monthly Tmax (c), mean monthly Tmin (e), and validation of monthly rainfall (b), mean monthly Tmax (d), mean monthly Tmin (f) for Mekelle AP station.

Rainfall projection on a monthly and/or seasonal basis is important for analysis of local impacts of climate variables than on an annual basis. In the Giba basin, the rainy season extends from mid-May to mid-September (MJJAS), and the summer season (JJA) is the main rainy season in which rainfed agriculture is intensively implemented. December to February (DJF) is the driest season, and irrigation practice is common in the basin from December to April (DJFMA).

In general, differences in rainfall projection are more pronounced among seasons than on an annual basis and are inconsistent between the RCPs. For instance, June rainfall for Abyi Adi station during the 2040s shows a relatively higher increase (up to +25, +30, and +45 mm for RCPs 2.6, 4.5, and 8.5, respectively) compared to July and August (Fig. 6a). The magnitude of increase of rainfall at Abyi Adi station will be higher in May and June than July and August in all RCPs for the whole projection period. However, this is not

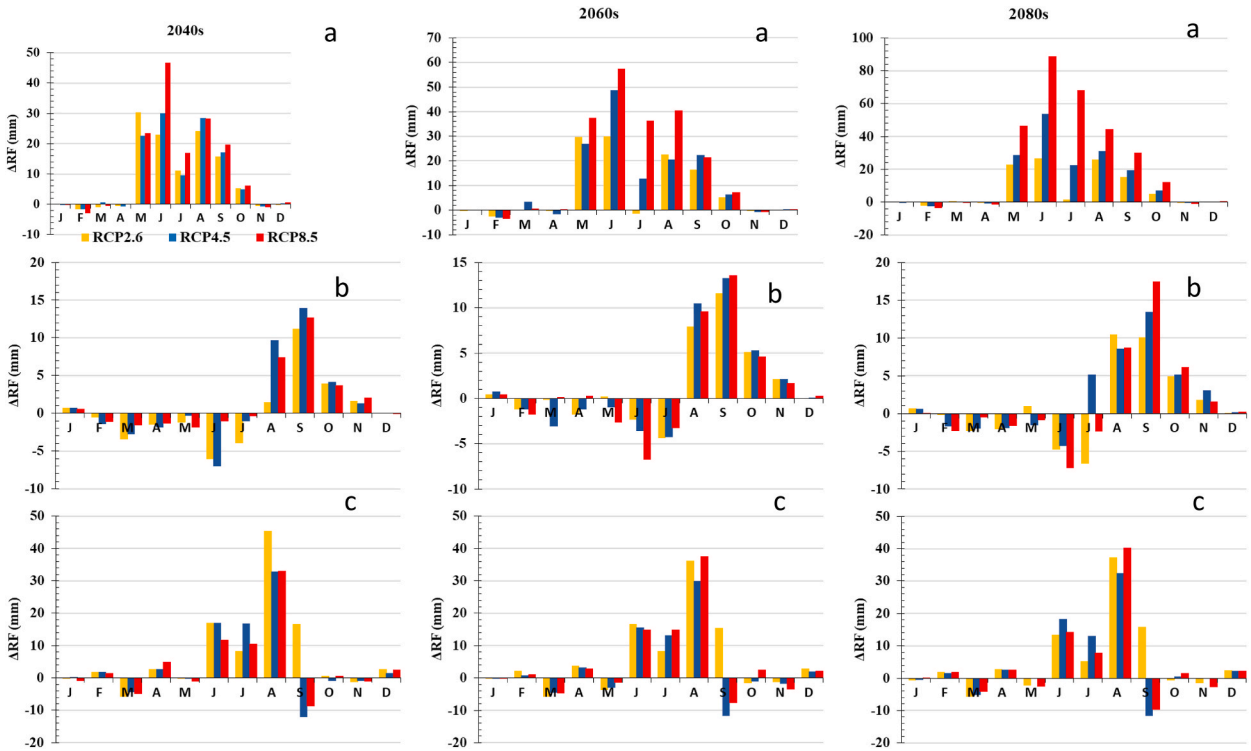

Fig. 6. Projected change of rainfall at Abyi Adi (a), Wukro (b), and Hagereselam (c) stations under RCPs (2.6, 4.5, 8.5) compared with historical data.

Table 6
Long-term change of annual rainfall and temperature projection for the 2040s, 2060s, and 2080s under three RCP scenarios compared to historical data.

Station	Variables	2040s			2060s			2080s		
		RCP 2.6	RCP 4.5	RCP 8.5	RCP 2.6	RCP 4.5	RCP 8.5	RCP 2.6	RCP 4.5	RCP 8.5
Hagereselam	RF	87.7	54.4	48.3	73.0	42.4	58.6	68.2	52.9	51.7
	Tmax	0.11	0.13	0.15	0.13	0.19	0.21	0.14	0.20	0.31
	Tmin	0.08	0.09	0.10	0.09	0.10	0.14	0.09	0.11	0.18
Abyi Adi	RF	106.4	110.4	137.7	99.8	136.3	198.2	95.7	158.7	284.5
	Tmax	0.11	0.13	0.15	0.13	0.19	0.21	0.14	0.20	0.31
	Tmin	0.95	1.01	1.17	1.04	1.23	1.69	1.00	1.36	2.35
Wukro	RF	2.3	15.3	19.0	17.6	17.8	16.2	13.0	24.8	19.3
	Tmax	−0.01	0.01	0.03	0.01	0.03	0.04	0.01	0.03	0.05
	Tmin	0.63	0.70	0.81	0.68	0.81	1.11	0.62	0.92	1.54
Fireweyni	RF	−9.6	−4.4	−2.5	4.1	38.3	−7.9	13.0	−3.0	44.2
	Tmax	−0.05	−0.07	−0.06	−0.08	−0.08	−0.09	−0.08	−0.08	−0.07
	Tmin	0.22	0.23	0.28	0.26	0.31	0.47	0.20	0.37	0.75
Hawzen	RF	41.0	29.6	59.3	41.7	44.0	78.6	28.0	59.2	119.6
	Tmax	−0.24	−0.30	−0.32	−0.30	−0.34	−0.43	−0.26	−0.33	−0.53
	Tmin	0.25	0.25	0.29	0.26	0.31	0.40	0.23	0.34	0.54
Mekelle AP	RF	49.2	52.7	72.7	65.8	70.8	118.2	50.0	90.6	208.5
	Tmax	−0.07	−0.09	−0.12	−0.09	−0.12	−0.24	−0.05	−0.17	−0.39
	Tmin	0.06	0.07	0.08	0.07	0.09	0.17	0.05	0.11	0.25
Mekelle Obs	RF	107.0	137.5	160.4	119.4	159.6	211.0	110.3	161.8	298.0
	Tmax	0.29	0.31	0.34	0.29	0.33	0.42	0.29	0.34	0.56
	Tmin	0.36	0.37	0.43	0.41	0.45	0.55	0.37	0.50	0.74

the case for Hagereselam station, where rainfall increase during JJA continues to be higher than other seasons for the whole projection (Fig. 6c). For the 2040s, rainfall at Hagereselam station is expected to increase up to +45 mm for August. Rainfall projection during MJJ for Wukro station is expected to slightly decrease (up to −9 mm) in all scenarios for the whole projection period (Fig. 6b). However, the overall trend of rainfall on an annual basis at this station shows an increasing trend, as the decrease in MJJ is

compensated by a relatively more increase during ASON that ranges from +20 mm in the 2040s under RCP 2.6 to about +35 mm in the 2080s under RCP 8.5.

A comparative change in seasonal projection of rainfall and temperature variables for all stations under the three scenarios till the end of the 21st century is presented in Annex 1. Seasonal analysis of projected rainfall in the basin shows that rainfall is expected to slightly decrease during the spring season (MAM) at Hagereselam, Wukro, Fireweyni, Hawzen, and Mekelle Obs stations under all scenarios for the whole analysis year (Annex 1). However, the projection of rainfall at Abyi Adi and Mekelle AP stations for the same season shows an increasing trend. For instance, seasonal rainfall during MAM (for Abyi Adi station) will increase by +29 and + 45 mm under RCP 2.6 and RCP 8.5 for the 2040s and 2080s, respectively. Seasonal projection of rainfall for the main rainy season (JJA) under RCP2.6 scenario for the projection years (2040s, 2060s, and 2080s) shows a significant increment at Hagereselam (+71, +61, +56 mm), Abyi Adi (+58, +51, +54 mm), Hawzen (+10, +8, +7 mm), Mekelle AP (+24, +32, +21 mm), and Mekelle Obs (+91, +102, +91 mm) stations. The projected increment of JJA rainfall for these stations is highest under RCP 8.5, in that for the same projection years, it increases by (+56, +68, +63 mm) at Hagereselam, (+92, +134, +202 mm) at Abyi Adi, (+23, +32, +54 mm) at Hawzen, (+38, +63, +114 mm) at Mekelle AP, and (+131, +168, +233 mm) at Mekelle Obs station. Different from this, rainfall during this season slightly decreases at Wukro and Fireweyni stations. Under the RCP 2.6 scenario, the range of rainfall increase varies from a minimum of +7 mm at Hawzen station for the 2080s to about +102 mm at Mekelle Obs station for the 2060s. Similarly, rainfall will increase up to a maximum of +137 mm (in 2060s) and +233 mm (in 2080s) at Mekelle Obs for RCPs 4.5 and 8.5, respectively. Rainfall projection for the autumn season (SON) shows an increasing trend up to +36 mm (2060s) under RCP 2.6 at Hawzen station, +42 mm and +81 mm (2080s) at Mekelle AP station under RCPs 4.5, and 8.5, respectively.

3.2.2. *Projection of future temperature*

On an annual basis, Tmax is expected to consistently rise at Hagereselam, Abyi Adi, Wukro, and Mekelle Obs stations for the three RCPs and the whole projection period. The trend of Tmax rise at these stations is consistent with respect to the RCPs and for the whole projection period. Contrary to this, Tmax is expected to fall at Fireweyni, Hawzen, and Mekelle AP stations for all RCPs and the projection period. Monthly changes of Tmax show diverging trends at all stations in the Giba basin. For instance, up to −0.5 °C fall in Tmax is expected in October, November, and December (OND) under all scenarios for the whole projection year at Abyi Adi station (Fig. 7a). This is in line with the analysis of historical temperature at Abyi Adi station (Fig. 2) that showed lower records of Tmax in these months compared to other months. At Wukro station, Tmax is expected to fall in August and OND during the projection period under all RCPs (Fig. 7b). The change of Tmax will decrease at Hagereselam station for May only (Fig. 7c).

Projections of Tmax for the Mekelle Obs show the highest increment compared to other stations in the Giba basin. At this station, Tmax is expected to increase by +0.29 °C in the 2040s and up to +0.56 °C in the 2080s under RCPs 2.6 and 8.5, respectively. On the

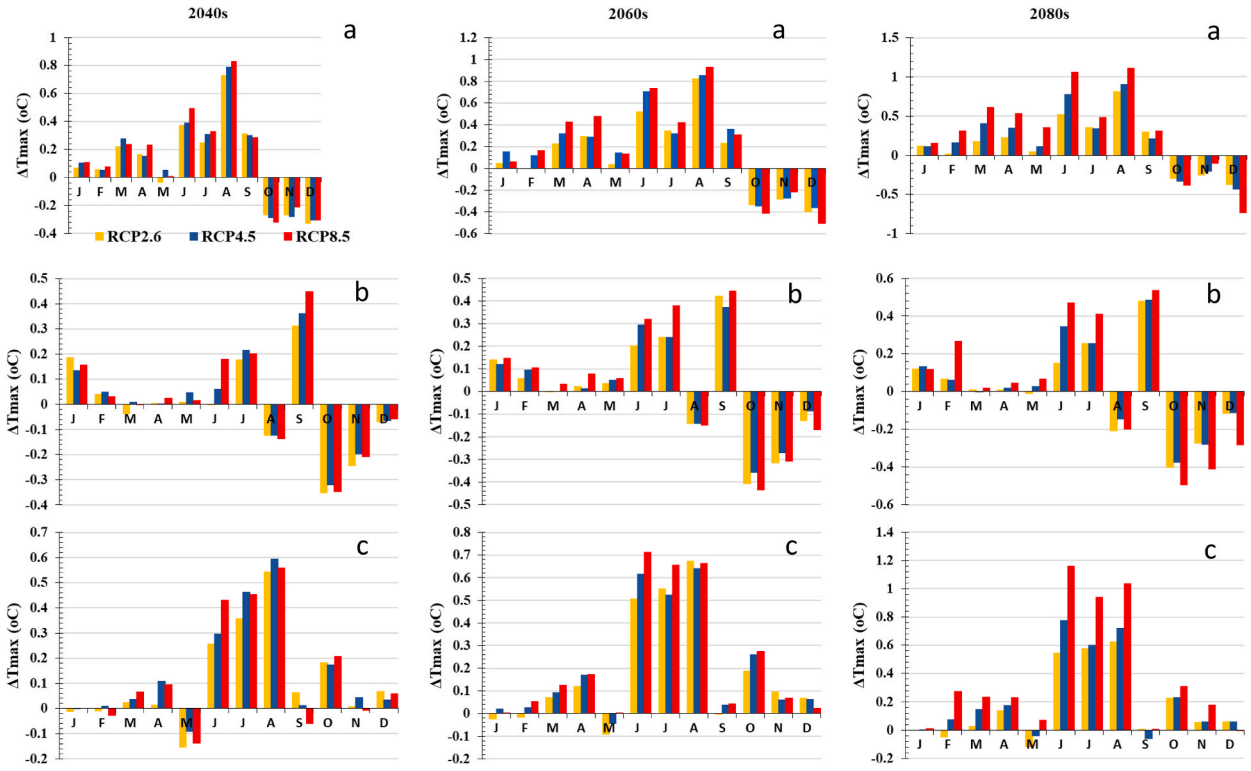

Fig. 7. Projected change of Tmax at Abyi Adi (a), Wukro (b), and Hagereselam (c) stations under RCPs (2.6, 4.5, 8.5) compared with historical data.

other hand, a relatively high decrease (up to −0.53 °C) of Tmax is projected for Hawzen station under RCP 8.5 for the 2080s.

Projected seasonal trends of Tmax are divergent among the stations. For instance, Tmax under RCP 2.6 for the 2040s is expected to decrease by up to −0.1 °C at Hawzen, Hagereselam, Abyi Adi, Wukro, and Fireweyni stations in DJF and MAM seasons. These seasons constitute the main irrigation months in the Giba basin. Hence, a relative fall of Tmax in these areas can be considered a favorable condition for irrigation water management as temperature fall contributes to lowering crop water evapotranspiration. For the main rainy season (JJA), Tmax is expected to decrease at Fireweyni and Hawzen stations, and significantly increase in the rest of the stations under RCP 2.6 for the 2040s. For the same scenario and projection period, Tmax in Autumn (SON) is expected to fall in the majority of the stations (e.g., Abyi Adi, Wukro, Fireweyni, Hawzen, and Mekelle AP) and slightly increase for the rest of the stations. In general, the projected seasonal change of Tmax for the 2040s under RCP 2.6 varies from a maximum decrease of −0.53 °C at Mekelle AP in SON to a maximum increase of +0.53 °C in JJA at Mekelle Obs.

Tmin is expected to increase in all stations under all scenarios for the whole projection year. Under the RCP 2.6 scenario, the projection of Tmin shows an inconsistent trend (between projection years), in which it rises during the 2060s compared to the 2040s, then slightly drops during the 2080s at all stations. However, it consistently rises for the whole analysis period under RCPs 4.5 and 8.5. On an annual basis, the range of Tmin increment varies from +0.06 °C under RCP 2.6 in the 2040s at Mekelle AP station to +2.35 °C at Abyi Adi station during the 2080s under RCP 8.5 (Table 6). Noting that Abyi Adi station has historical records of the highest temperature in the Giba basin, this projection of the highest rise of Tmin suggests that hotter areas will get hotter in the future. Even under RCP 2.6, Tmin in Abyi Adi station will rise by +0.95 and + 1.04 °C during the 2040s and 2060s, respectively.

On a monthly basis, Tmin increases in all months except in December at Abyi Adi station (Fig. 8a), decreases in January, February, April and May at Wukro station (Fig. 8b), and in February, April, May, August, and November at Hagereselam station (Fig. 8c) under all RCPs for the whole projection year. This implies the trend of Tmin on monthly basis is differing and inconsistent among the stations in the basin.

Under RCP 2.6 for the 2040s, Tmin in DJF and MAM slightly decreases at Hagereselam, Wukro, Hawzen, Mekelle AP and Mekelle Obs stations, and increases in the rest of the stations (Annex 1). The maximum change of Tmin in these seasons reaches up to −0.26 °C fall in MAM at Wukro station, and up to +0.76 °C rise in the same season at Abyi Adi station. For the same projection year, Tmin significantly increases in all stations in JJA and SON seasons. For instance, Tmin will increase up to +1.6 °C at Wukro and up to +1.98 °C at Abyi Adi stations in JJA and SON seasons respectively during the 2040s under RCP 2.6. In general, it is observed that the rate of increment of projected Tmin is more than that of Tmax in all stations in the Giba basin. This is in agreement with the historical (decadal) climate analysis in Ethiopia [58], which reported a remarkably increasing trend of minimum temperature values during the last 3-5 decades. This shows that the gap between Tmin and Tmax will get narrower, which is also an indicator of global warming [59]. The findings of the present study are in line with other studies carried out at global and regional scales. For instance, Easterling et al. [60] reported that the diurnal temperature range continues to narrow in most parts of the world, particularly for much of the Southern

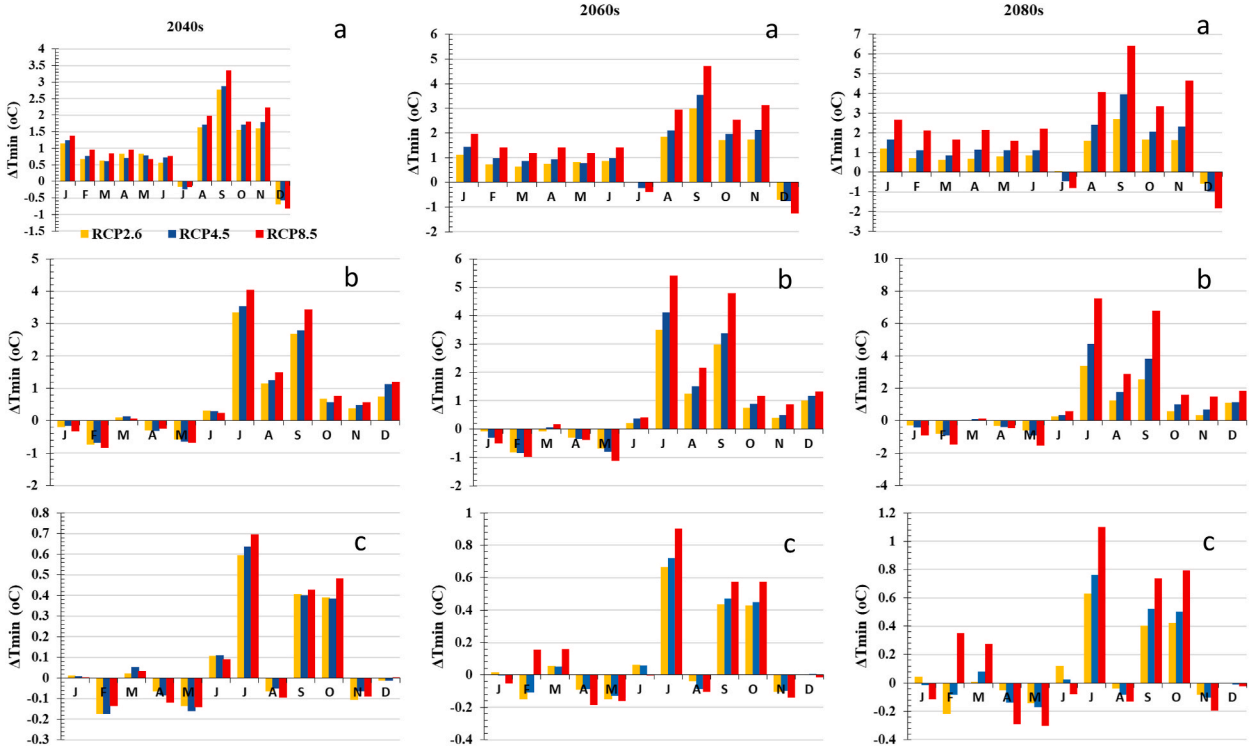

Fig. 8. Projected change of Tmin at Abyi Adi (a), Wukro (b), and Hagereselam (c) stations under RCPs (2.6, 4.5, 8.5) compared with historical data.

Hemisphere. Similarly, global studies e.g., Alexander et al. [61] and regional studies e.g., Martín et al. [62] noted the significant change in long-term minimum temperature extremes than maximum temperature extremes throughout the 21st century.

The effect of elevation on temperature and rainfall variability was assessed in this study. Temperature lapse rate per 1000 m elevation differences were calculated for the historical and projected temperature variability in the basin. In this regard, historical mean annual temperature variability showed a strong correlation with elevation (Fig. 9a). The historical mean annual maximum and minimum temperature lapse rates are significantly different with 8.6 °C/1000 m and 2.6 °C/1000 m, respectively. The mean annual temperature lapse rate in the Giba basin is 5.6 °C/1000 m. This is nearly similar to the national average of Ethiopia, which is about 5.8 °C/1000 [58].

However, the correlation between mean annual rainfall and elevation is extremely weak ($R^2 = 0.18$) in the basin. Long-term mean annual rainfall has no clear trend with respect to altitudinal differences of the meteorological stations in the basin (Table 1, Fig. 9b).

Long-term analysis of historical meteorological data showed that elevation is a main parameter influencing temperature in the Giba basin (Fig. 9a). Similarly, the influence of elevation on the projected changes of long-term mean annual Tmin was also reflected by intermediate correlation ($R^2 = 0.66$) (Fig. 10b).

However, the influence of elevation on the projected changes of long-term mean annual Tmax and rainfall was identified by extremely poor correlation ($R^2 = 0.08$) (Fig. 10a and c). Fazzini et al. [58] reported that local physiographic factors such as topography and aspect play a key role in the variability of rainfall in Ethiopia. The evidence that shows the insignificant variations of projected changes of Tmax values irrespective of the altitudinal differences of the meteorological stations is witnessed in the majority of the stations in the Giba basin. For instance, the Abyi Adi and Hagereselam stations have altitudinal differences of about 791 m (Table 1). However, the projected change of Tmax for the 2040s under the RCP 2.6 is equal, i.e.,0.11 °C (Table 6). Similarly, in the same projection period, the changes of projected Tmax for the Fireweyni and Wukro stations, which have altitudinal differences of about 483 m, are nearly the same, i.e., −0.05 and −0.01 °C respectively. Hence, it can be arguably concluded that elevation has little impact on the variations of changes of projected long-term mean annual Tmax and rainfall, but intermediate impact in Tmin variability in the Giba basin.

3.3. Climate indices

For the first time in the Giba basin, the De Martonne Aridity and Pinna Combinative Indices were calculated for the historical and future periods under the three RCPs. The De Martonne Aridity Index result shows that the majority of parts of the Giba basin are classified as semi-arid under the three time periods.

Comparing the historical and projected rainfall and temperature variables in the study area, the monthly De Martonne Aridity Index shows varied results among the stations and months. The range of change of the De Martonne Aridity Index for Abyi Adi station is expected to considerably increase from 51 % in 2040s under RCP 2.6 (Fig. 11a1) up to 114 % in 2080s under RCP 8.5 (Fig. 11a3). September and October are months of peak De Martonne Aridity Index at Abyi Adi station. This is in line with the projection for September that Tmin is expected to considerably rise under the three scenarios for the whole projection period (Fig. 8a). However, it is different at Hagereselam station in that aridity index in September is expected to decrease under all RCPs for the whole projection year (Fig. 11b). This is because the change of Tmax for September is insignificant for the whole projection period under all RCPs at Hagereselam station (Fig. 7c). At Wukro station, maximum aridity index in SON is expected to vary from 59 % in the 2040s under RCP 2.6 (Fig. 11c1), to 128 % under RCP 4.5 in the 2080s (Fig. 11c3). This is attributed to the high increment of Tmin under all RCPs for the whole projection period (Fig. 8b). The increase of aridity index in the main rain season (JJA) is insignificant as the magnitude of increase of rainfall in these months is considerably higher than that of average temperature. However, it showed significant increment during the Autumn season (SON) and diverging trends in the Winter (DJF) and Spring (MAM) seasons (Fig. 11 a-c). Hence, it can be noted that the level of aridity highly varies even under finer spatiotemporal scales in the Giba basin. In line with these findings, Gebremedhin et al. [63] applied the De Martonne aridity index, Pinna combinative index, and the Food and Agriculture Organization aridity index methods, and reported high spatiotemporal variability of aridity in the Raya Valley in northern Ethiopia. Hence, this calls for site-specific interventions that are adjusted according to changes in the trends and spatiotemporal patterns of aridity.

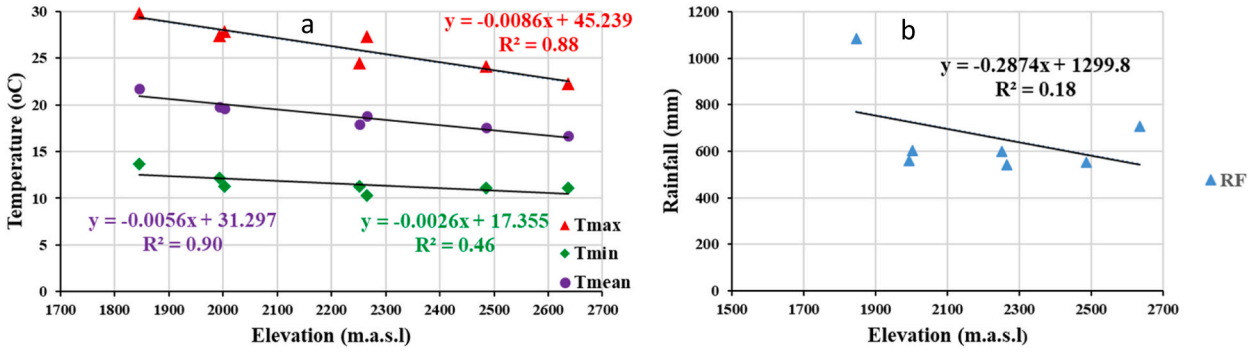

Fig. 9. Lapse rate for maximum, minimum, and mean temperature (a) and correlation of rainfall and elevation (b) in the Giba basin.

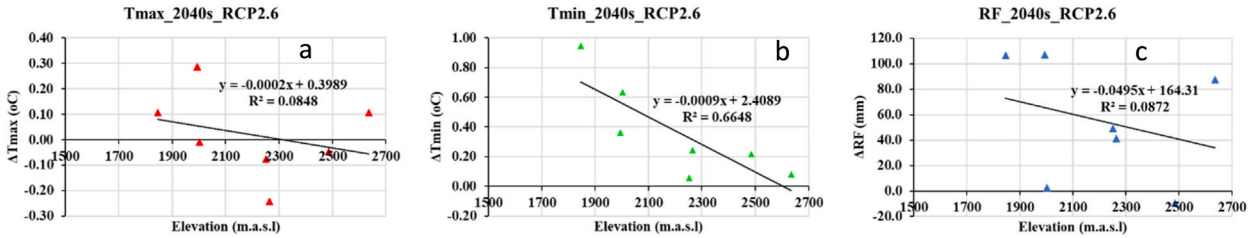

Fig. 10. Correlation of projected change of Tmax (a), Tmin (b), and rainfall (c) during the 2040s under RCP 2.6 in the Giba basin.

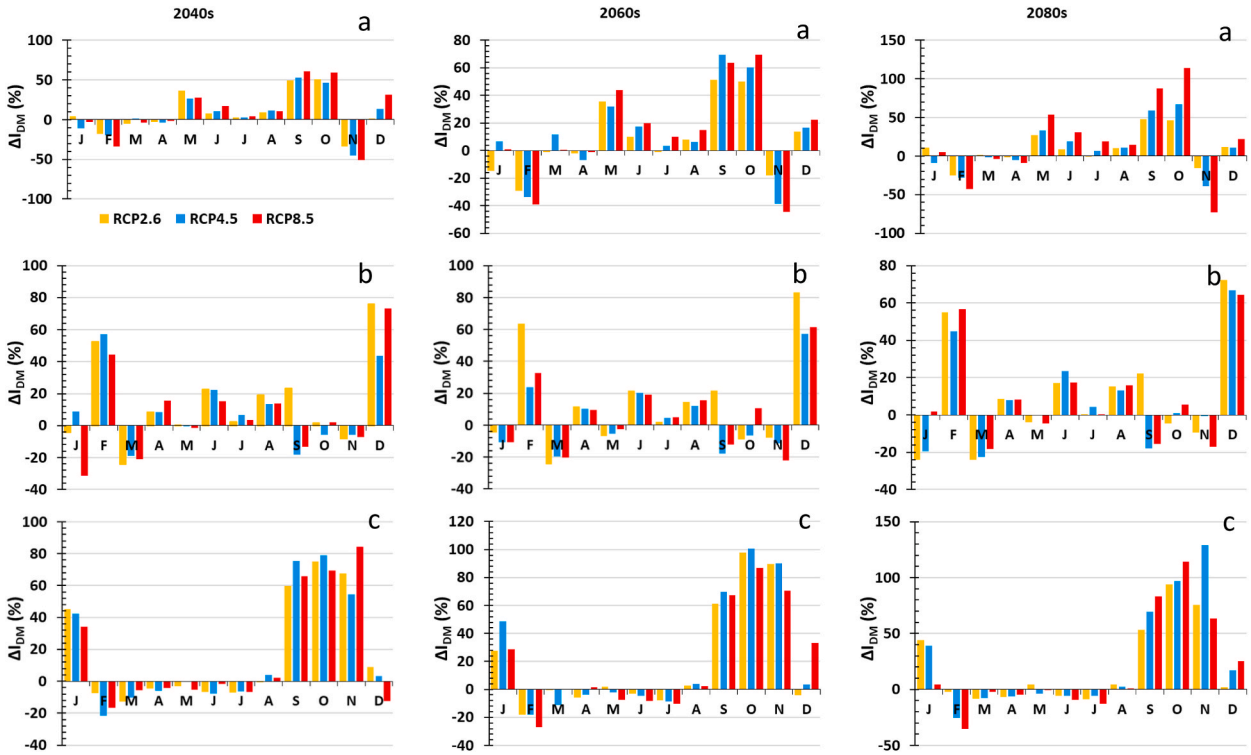

Fig. 11. Projection of Monthly De Martonne Aridity Indices at Abyi Adi (a), Hagereselam (b), and Wukro (c) stations under RCPs (2.6, 4.5, 8.5) compared with historical data.

The Pinna Combinative Aridity Index for all stations in the Giba basin shows a similar trend to the De Martonne Aridity Index. Pinna Combinative Index significantly increases under RCP 8.5 compared to RCPs 2.6 and 4.5. For instance, change of Pinna Combinative Index for Mekelle Obs varies from 16 % under RCP 2.6 (Fig. 12a) and 25 % under RCP 4.5 (Fig. 12b) to about 47 % under RCP 8.5 (Fig. 12c). The trend is similar at all stations except some variation with respect to the magnitude of change. In general, the two methods for the projection of aridity index show a very high correlation coefficient (Fig. 12), which indicates the good performance of the methods. However, the De Martonne Aridity Index was found more advantageous for the current study since it can be computed at finer temporal resolution (including on a monthly and seasonal basis) which is helpful for irrigation scheduling and water resources management. Overall, the two methods show that aridity will considerably increase till the end of the 21st century under the three emission scenarios in the Giba basin. This leads to crop water deficiency, particularly during irrigation seasons.

The findings of the current study are in line with other studies in semi-arid regions around the globe, e.g., an increase of De Martonne and Pinna combinative aridity indices was reported in northern Ethiopia [63], South India [64], Iran [65,66], Turkey [28], southwestern Spain [56], and northern Greece [57], among others. In line with this, Zarch et al. [67] also projected that the areal extent of hyper-arid, arid, and semi-arid zones will increase by 7.46 %, 7.01 %, and 5.80 %, respectively from 2006 to 2100 at a global scale.

4. Conclusion

This study investigates historical and future climate change trends in the Giba basin, northern Ethiopia. It has also demonstrated

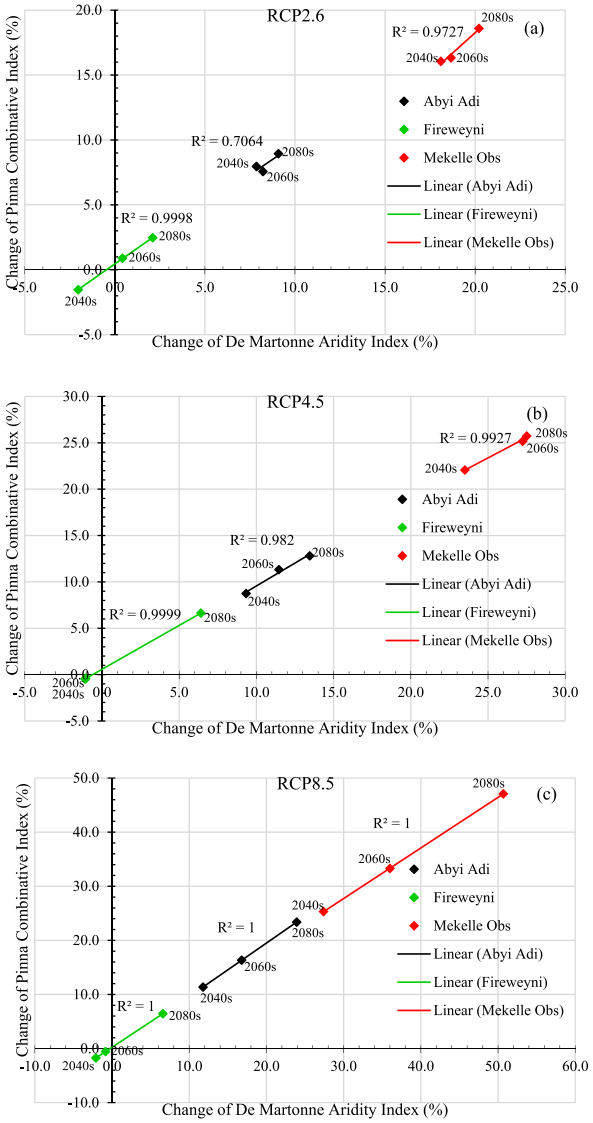

Fig. 12. Correlation of De Martonne Aridity Index and Pinna Combinative Index for Abyi Adi, Fireweyni, and Mekelle Obs stations under RCP 2.6 (a), RCP 4.5 (b), and RCP 8.5 (c) scenarios for the 2040s, 2060s, and 2080s projection period.

the applicability of De Martonne and Pinna Combinative aridity indices for the first time in the basin. This will certainly provide useful information for agricultural extension workers and policymakers who take role of planning and implementing climate change mitigation and adaptation measures in the basin. This study considerably improves our understanding of long-term climate variability accompanied by aridity dynamics so as to trigger resilience-building initiatives for addressing climate change impacts on the environment in general. This study has noted that analysis of rainfall and temperature variability on a monthly and/or seasonal basis is more useful than the annual basis for impact studies, e.g., for irrigation scheduling and water management in areas where irrigation practices are becoming promising remedies for ensuring food security in the Giba basin. In this regard, seasonal analysis of projected rainfall in the basin shows that rainfall is expected to slightly decrease (accompanied by a significant increase in Tmax) during the spring season (MAM) at Hagereselam, Wukro, Fireweyni, Hawzen, and Mekelle Obs stations under all scenarios for the whole analysis year. This implies crop water deficit during the irrigation season will be increased in the majority areas of the basin. Projection of rainfall for the main rainy season (JJA) shows a significant increment in the majority of the stations in the Giba basin, which considerably varies from a minimum of +10 mm under RCP2.6 for the 2040s at Hawzen station to a maximum of +233 mm under RCP8.5 for the 2080s at Mekelle Obs station. At the same season, projections of Tmax for Mekelle Obs shows highest increment (+0.29 °C in the 2040s and up to +0.56 °C in the 2080s under RCPs 2.6 and 8.5, respectively) compared to other stations in the basin. This threatens the adequacy of rainfall for rainfed crops in the Mekelle area as the relatively higher temperature rise during the rainy season will induce higher evapotranspiration rates.

On an annual basis, Tmax is expected to consistently rise at the majority of the stations in the basin under the three RCPs and for the

whole projection period. Similarly, Tmin is expected to increase in all stations under all scenarios for the whole projection year. On an annual basis, the range of Tmin increment varies from +0.06 °C under RCP 2.6 in the 2040s at Mekelle AP station to +2.35 °C at Abyi Adi station during the 2080s under RCP 8.5. In general, it is noticeable that the magnitude of change of temperature is more pronounced than that of rainfall throughout the Giba basin during the last decades and the same trend will continue till the end of the 21st century. In addition, it can be concluded that the rate of increment of projected Tmin is more than that of Tmax in all stations in the Giba basin, which shows a contraction of the gap between Tmin and Tmax. On top of this, it is also observed that hotter areas (mainly low-lying areas of the basin) will get more hotter in the future. Hence, these all indicate the prevalence of global warming in the basin. The analysis of long-term projected changes in mean annual temperature and rainfall variability showed that elevation has little impact on the variations of changes of projected long-term mean annual Tmax and rainfall, but intermediate impact in Tmin variability in the Giba basin.

The De Martonne and Pinna Combinative aridity index results show that the majority of parts of the Giba basin are classified as semi-arid environments throughout the whole projection period. More specifically, the De Martonne aridity index has paramount importance for the assessment of aridity conditions in areas where irrigation practices are common, as it is capable of indicating the frequency of irrigation in a specific month and/or season. In general, aridity will considerably increase till the end of the 21st century under the three emission scenarios in the basin. Hence, the implementation of locally suited climate change resilient strategies is crucial to maintain the sustainability of the ecosystem and ensuring food security in the basin.

CRediT authorship contribution statement

Atsbha Brhane Gebru: Writing – original draft, Visualization, Validation, Software, Methodology, Formal analysis, Data curation, Conceptualization. **Tesfamichael Gebreyohannes:** Writing – review & editing, Supervision, Conceptualization. **Gebrerufael Hailu Kahsay:** Writing – review & editing.

Ethics statement

This study does not involve any human or animal subjects, and it is in accordance with research ethical standards.

Data availability statement

Data will be made available on request. For requesting data, please write to the corresponding author.

Funding statement

This research did not receive any grants from funding agencies or organizations.

Declaration of competing interest

The authors declare that they have no known competing financial interests or personal relationships that could have appeared to influence the work reported in this paper.

Annex 1. Long-term change of seasonal projection of rainfall, Tmax, and Tmin variables in the Giba basin

Station	Variables	Seasons	2040s			2060s			2080s		
			RCP 2.6	RCP 4.5	RCP 8.5	RCP 2.6	RCP 4.5	RCP 8.5	RCP 2.6	RCP 4.5	RCP 8.5
Hagereselam	RF	DJF	4.3	3.7	3.1	4.9	2.5	3.0	3.7	3.3	4.3
		MAM	−3.3	−2.0	−1.1	−5.7	−4.3	−3.2	−5.2	−2.9	−4.2
		JJA	70.7	66.8	55.5	61.2	58.7	67.6	56.0	63.8	62.5
		SON	15.9	−14.0	−9.2	12.6	−14.5	−8.8	13.7	−11.4	−10.9
	Tmax	DJF	0.01	0.01	0.01	0.01	0.04	0.03	0.00	0.05	0.09
		MAM	−0.04	0.02	0.01	0.03	0.07	0.10	0.02	0.09	0.18
		JJA	0.39	0.45	0.48	0.58	0.59	0.68	0.59	0.70	1.05
		SON	0.09	0.08	0.05	0.09	0.12	0.13	0.10	0.08	0.17
	Tmin	DJF	−0.06	−0.06	−0.04	−0.04	−0.04	0.03	−0.06	−0.04	0.07
		MAM	−0.06	−0.06	−0.08	−0.06	−0.05	−0.06	−0.06	−0.07	−0.11
		JJA	0.21	0.23	0.23	0.23	0.23	0.27	0.24	0.23	0.30
		SON	0.23	0.24	0.27	0.25	0.27	0.34	0.25	0.31	0.45
Abyi Adi	RF	DJF	−1.4	−1.6	−2.3	−2.6	−2.4	−2.9	−1.6	−2.4	−3.0
		MAM	29.0	22.7	23.1	29.7	28.6	38.6	23.4	27.8	44.8
		JJA	58.3	68.1	91.9	51.2	82.1	134.4	54.1	107.5	201.7

(*continued on next page*)

(*continued*)

Station	Variables	Seasons	2040s			2060s			2080s		
			RCP 2.6	RCP 4.5	RCP 8.5	RCP 2.6	RCP 4.5	RCP 8.5	RCP 2.6	RCP 4.5	RCP 8.5
		SON	20.6	21.2	25.0	21.5	27.9	28.0	19.9	25.7	41.0
	Tmax	DJF	−0.07	−0.05	−0.04	−0.12	−0.03	−0.09	−0.08	−0.05	−0.09
		MAM	0.12	0.16	0.16	0.19	0.25	0.35	0.15	0.29	0.50
		JJA	0.45	0.50	0.55	0.57	0.63	0.70	0.57	0.68	0.89
		SON	−0.08	−0.09	−0.08	−0.13	−0.09	−0.11	−0.09	−0.11	−0.06
	Tmin	DJF	0.37	0.48	0.51	0.38	0.56	0.69	0.45	0.61	0.98
		MAM	0.76	0.70	0.82	0.74	0.86	1.26	0.71	1.04	1.79
		JJA	0.68	0.73	0.86	0.90	0.95	1.32	0.84	1.02	1.82
		SON	1.98	2.13	2.47	2.15	2.55	3.46	2.00	2.78	4.80
Wukro	RF	DJF	0.3	−0.7	−0.7	−0.8	−0.4	−1.1	0.5	−0.9	−2.1
		MAM	−6.2	−5.0	−4.8	−1.7	−5.2	−2.2	−3.4	−5.5	−2.9
		JJA	−8.6	1.6	6.0	1.2	2.6	−0.5	−1.0	9.5	−0.9
		SON	16.8	19.5	18.4	18.9	20.8	19.9	16.8	21.8	25.2
	Tmax	DJF	0.05	0.04	0.04	0.02	0.04	0.03	0.02	0.03	0.04
		MAM	−0.01	0.02	0.01	0.02	0.02	0.06	0.00	0.02	0.05
		JJA	0.02	0.05	0.08	0.10	0.13	0.18	0.07	0.15	0.23
		SON	−0.10	−0.05	−0.04	−0.10	−0.09	−0.10	−0.07	−0.06	−0.12
	Tmin	DJF	−0.06	0.10	0.01	0.03	0.01	−0.05	0.00	−0.07	−0.19
		MAM	−0.26	−0.27	−0.29	−0.36	−0.37	−0.44	−0.31	−0.40	−0.63
		JJA	1.60	1.69	1.93	1.66	2.00	2.66	1.63	2.29	3.68
		SON	1.25	1.28	1.59	1.38	1.59	2.28	1.16	1.84	3.30
Fireweyni	RF	DJF	7.1	4.5	5.9	7.9	6.8	3.9	7.2	6.7	4.6
		MAM	−5.3	1.1	−0.8	−6.0	−5.6	−3.7	−6.1	1.6	−1.1
		JJA	−16.2	−12.5	−14.9	−7.6	15.4	−14.5	−1.2	−15.0	22.8
		SON	4.8	2.6	7.3	9.9	21.7	6.4	12.9	3.7	17.9
	Tmax	DJF	0.01	−0.04	−0.06	−0.06	−0.10	−0.06	−0.04	−0.08	−0.08
		MAM	−0.03	−0.02	−0.03	−0.01	−0.05	−0.02	−0.03	0.01	0.03
		JJA	−0.05	−0.05	−0.04	−0.09	−0.03	−0.13	−0.09	−0.10	−0.06
		SON	−0.12	−0.15	−0.12	−0.17	−0.14	−0.16	−0.16	−0.15	−0.16
	Tmin	DJF	0.37	0.34	0.38	0.40	0.38	0.64	0.28	0.45	0.86
		MAM	−0.03	0.04	0.09	0.08	0.12	0.24	0.00	0.17	0.55
		JJA	0.16	0.19	0.27	0.15	0.30	0.41	0.15	0.35	0.69
		SON	0.38	0.36	0.39	0.40	0.44	0.57	0.36	0.50	0.89
Hawzen	RF	DJF	−1.0	−1.2	−0.3	−1.7	−2.4	−3.5	−0.8	−1.8	−4.5
		MAM	−1.4	−0.2	−1.6	−0.8	−3.5	−0.6	−1.9	−3.1	−7.7
		JJA	10.3	1.8	22.7	7.8	13.7	32.4	7.1	23.5	53.9
		SON	33.1	29.2	38.4	36.4	36.1	50.3	23.6	40.6	77.8
	Tmax	DJF	0.02	−0.05	0.03	0.01	0.05	0.13	−0.01	0.04	0.15
		MAM	−0.10	−0.17	−0.17	−0.14	−0.16	−0.25	−0.12	−0.17	−0.31
		JJA	−0.48	−0.49	−0.64	−0.59	−0.69	−0.91	−0.50	−0.62	−1.04
		SON	−0.41	−0.48	−0.48	−0.49	−0.55	−0.71	−0.43	−0.56	−0.90
	Tmin	DJF	−0.02	−0.03	−0.02	−0.03	−0.02	0.02	−0.03	−0.01	0.03
		MAM	−0.02	0.00	0.03	0.03	0.05	0.11	−0.01	0.07	0.27
		JJA	0.19	0.18	0.24	0.21	0.21	0.25	0.19	0.21	0.31
		SON	0.84	0.85	0.91	0.85	1.00	1.21	0.77	1.10	1.56
Mekelle AP	RF	DJF	−4.2	−4.2	−3.9	−4.3	−4.6	−1.6	−4.5	−3.9	−1.1
		MAM	1.9	6.1	5.5	5.7	7.2	7.4	8.7	8.4	15.6
		JJA	23.5	26.2	38.0	32.2	32.9	62.8	21.3	44.6	113.5
		SON	28.0	24.7	33.0	32.2	35.3	49.6	24.4	41.6	80.6
	Tmax	DJF	0.05	0.05	0.05	0.04	0.06	−0.11	0.09	0.00	−0.24
		MAM	0.03	−0.04	−0.08	−0.04	−0.08	−0.25	0.01	−0.13	−0.50
		JJA	0.15	0.17	0.18	0.21	0.16	0.22	0.24	0.14	0.25
		SON	−0.53	−0.56	−0.61	−0.56	−0.63	−0.81	−0.55	−0.70	−1.07
	Tmin	DJF	0.00	0.00	0.01	0.00	0.05	0.24	−0.04	0.09	0.39
		MAM	−0.03	−0.01	0.00	−0.03	−0.01	0.06	−0.03	0.01	0.12
		JJA	0.06	0.09	0.06	0.08	0.07	0.08	0.07	0.08	0.09
		SON	0.20	0.21	0.24	0.22	0.25	0.30	0.20	0.27	0.41
Mekelle Obs	RF	DJF	−0.5	−0.2	−1.1	−0.3	−0.5	−0.6	−1.5	−0.8	−0.5
		MAM	−5.6	0.1	−4.3	−6.7	−4.2	−7.5	−2.4	−5.4	−9.4
		JJA	90.5	106.2	130.7	101.9	136.7	167.9	90.8	135.7	232.9
		SON	22.6	31.5	35.1	24.4	27.6	51.1	23.3	32.3	75.0
	Tmax	DJF	0.16	0.19	0.17	0.11	0.18	0.14	0.14	0.20	0.14
		MAM	0.14	0.15	0.17	0.14	0.19	0.25	0.14	0.16	0.29
		JJA	0.53	0.55	0.60	0.53	0.59	0.72	0.57	0.57	1.06
		SON	0.32	0.36	0.41	0.37	0.38	0.58	0.33	0.42	0.76
	Tmin	DJF	−0.22	−0.21	−0.24	−0.22	−0.22	−0.34	−0.25	−0.25	−0.42
		MAM	−0.01	0.03	0.07	0.05	0.02	0.17	−0.02	0.08	0.18

(*continued on next page*)

(*continued*)

Station	Variables	Seasons	2040s			2060s			2080s		
			RCP 2.6	RCP 4.5	RCP 8.5	RCP 2.6	RCP 4.5	RCP 8.5	RCP 2.6	RCP 4.5	RCP 8.5
		JJA	0.67	0.70	0.76	0.71	0.81	1.05	0.72	0.89	1.49
		SON	1.02	0.96	1.13	1.11	1.17	1.33	1.03	1.29	1.72

References

[1] S.H. Gebrechorkos, C. Bernhofer, S. Hülsmann, Climate change impact assessment on the hydrology of a large river basin in Ethiopia using a local-scale climate modelling approach, Sci. Total Environ. 742 (2020), https://doi.org/10.1016/j.scitotenv.2020.140504.

[2] S.H. Gebresellase, Z. Wu, H. Xu, W.I. Muhammad, Evaluation and selection of CMIP6 climate models in upper Awash basin (UBA), Ethiopia, Theor. Appl. Climatol. 149 (2022) 1521–1547, https://doi.org/10.1007/s00704-022-04056-x.

[3] M.A. Gurara, N.B. Jilo, A.D. Tolche, A.K. Kassa, Climate change projection using the statistical downscaling model in Modjo watershed , upper Awash River Basin , Ethiopia, Int. J. Environ. Sci. Technol. 19 (2022) 8885–8898, https://doi.org/10.1007/s13762-021-03752-x.

[4] H. Birara, R.P. Pandey, S.K. Mishra, Projections of future rainfall and temperature using statistical downscaling techniques in Tana Basin , Ethiopia, Sustain. Water Res. Manag. 6 (2020), https://doi.org/10.1007/s40899-020-00436-1.

[5] G. Gebremeskel, A. Kebede, Estimating the effect of climate change on water resources : integrated use of climate and hydrological models in the Werii watershed of the Tekeze River Estimating the effect of climate change on water resources : integrated use of climate and hydrologic, Agri. Nat. Res. (2018) 1–13, https://doi.org/10.1016/j.anres.2018.06.010.

[6] M.B. Hailu, H.S.K. Mishra, S.K. Jain, V.P. Singh, Evaluation and application of SDSM to assess the projected climate change effects on the Tekeze watershed , Ethiopia, Model. Earth Sys. Environ. (2022), https://doi.org/10.1007/s40808-022-01566-5.

[7] M.A. Gebremedhin, A.Z. Abraha, A.A. Fenta, Changes in future climate indices using Statistical Downscaling Model in the upper Baro basin of Ethiopia, Theor. Appl. Climatol. (2017), https://doi.org/10.1007/s00704-017-2151-4.

[8] S.H. Gebrechorkos, S. Hülsmann, C. Bernhofer, Changes in temperature and precipitation extremes in Ethiopia, Int. J. Climatol. 39 (2019) 18–30, https://doi.org/10.1002/joc.5777.

[9] A.A. Mekonen, A.B. Berlie, Spatiotemporal variability and trends of rainfall and temperature in the Northeastern highlands of Ethiopia, Model. Earth Sys. Environ. 6 (2020) 285–300, https://doi.org/10.1007/s40808-019-00678-9.

[10] U. Adhikari, A. Nejadhashemi, S. Woznicki, Climate change and eastern Africa: a review of impact on major crops, Food Energy Secur. 4 (2015) 110–132, https://doi.org/10.1002/fes3.61.

[11] S.H. Gebrechorkos, S. Hülsmann, C. Bernhofer, Regional climate projections for impact assessment studies in East Africa, Environ. Res. Lett. 14 (2019), https://doi.org/10.1088/1748-9326/ab055a.

[12] M. Amirabadizadeh, A.H. Ghazali, Y.F. Huang, A. Wayayok, Downscaling daily precipitation and temperatures over the Langat River Basin in Malaysia: a comparison of two statistical downscaling approaches, Int. J. Water Resour. Environ. Eng. 8 (2016) 120–136, https://doi.org/10.5897/IJWREE2016.0585.

[13] A. Asfaw, B. Simane, A. Hassen, A. Bantider, Variability and time series trend analysis of rainfall and temperature in northcentral Ethiopia: a case study in Woleka sub-basin, Weather Clim. Extrem. 19 (2018) 29–41, https://doi.org/10.1016/j.wace.2017.12.002.

[14] A.A. Shawul, S. Chakma, Trend of extreme precipitation indices and analysis of long-term climate variability in the Upper Awash basin , Ethiopia, Theor. Appl. Climatol. (2020), https://doi.org/10.1007/s00704-020-03112-8.

[15] M.T. Tadese, L. Kumar, R. Koech, B. Zemadim, Hydro-climatic variability : a characterisation and trend study of the awash river basin , Ethiopia, Hydrology 6 (2019), https://doi.org/10.3390/hydrology6020035.

[16] G.G. Haile, Q. Tang, S.-M. Hosseini-Moghari, X. Liu, T.G. Gebremicael, G. Leng, A. Kebede, X. Xu, X. Yun, Projected Impacts of Climate Change on Drought Patterns over East Africa, American Geophysical Union, 2020, https://doi.org/10.1029/2020EF001502.

[17] S. Pervez, G. Henebry, Projections of the Ganges–Brahmaputra precipitation—downscaled from GCM predictors, J. Hydrol. (2014), https://doi.org/10.1016/j.jhydrol.2014.05.016.

[18] K.W. Dixon, J.R. Lanzante, M.J. Nath, K. Hayhoe, A. Stoner, A. Radhakrishnan, V. Balaji, C.F. Gaitán, Evaluating the stationarity assumption in statistically downscaled climate projections: is past performance an indicator of future results? Clim. Change 135 (2016) 395–408, https://doi.org/10.1007/s10584-016-1598-0.

[19] R. Meenu, S. Rehana, P. Mujumdar, Assessment of hydrologic impacts of climate change in Tunga–Bhadra river basin, India with HEC-HMS and SDSM, Hydrol. Process. 27 (2013) 1572–1589, https://doi.org/10.1002/hyp.9220.

[20] A.F. Lutz, H.W. ter Maat, H. Biemans, A.B. Shrestha, P. Wester, W.W. Immerzeel, Selecting representative climate models for climate change impact studies: an advanced envelope-based selection approach, Int. J. Climatol. 36 (2016) 3988–4005, https://doi.org/10.1002/joc.4608.

[21] R.L. Wilby, C. Dawson, Sdsm — a decision support tool for the assessment of regional climate change impacts, Environ. Model. Software 17 (2004) 145–157, https://doi.org/10.1016/S1364-8152(01)00060-3.

[22] P. Coulibaly, Y.B. Dibike, F. Anctil, Downscaling precipitation and temperature with temporal neural networks, J. Hydrometeorol. 6 (2005) 483–496, https://doi.org/10.1175/JHM409.1.

[23] H. Tavakol-Davani, M. Nasseri, B. Zahraie, Improved statistical downscaling of daily precipitation using SDSM platform and data-mining methods, Int. J. Climatol. 33 (2012) 2561–2578, https://doi.org/10.1002/joc.3611.

[24] J.M. Eden, M. Widmann, D. Grawe, S. Rast, Skill, correction, and downscaling of GCM-simulated precipitation, J. Climatol. 25 (2012) 3970–3984, https://doi.org/10.1175/JCLI-D-11-00254.1.

[25] R.L. Wilby, C.W. Dawson, The Statistical DownScaling Model : insights from one decade, Int. J. Climatol. 33 (2013) 1707–1719, https://doi.org/10.1002/joc.3544.

[26] C.M. Goodess, C. Anagnostopoulou, A. Bárdossy, C. Frei, C. Harpham, M.R. Haylock, Y. Hundecha, P. Maheras, J. Ribalaygua, J. Schmidli, T. Schmith, K. Tolika, R. Tomozeiu, An intercomparison of statistical downscaling methods for Europe and European regions – assessing their performance with respect to extreme temperature and precipitation events, Environ. Sci. (2012).

[27] H.J. Fowler, R.L. Wilby, Beyond the downscaling comparison study, Int. J. Climatol. 27 (2007) 1543–1545, https://doi.org/10.1002/joc.1616.

[28] A. Deniz, H. Toros, S. Incecik, Spatial variations of climate indices in Turkey, Int. J. Climatol. 31 (2011) 394–403, https://doi.org/10.1002/joc.2081.

[29] M. Montazerolghaem, W. Vervoort, B. Minasny, A. McBratney, Spatiotemporal monthly rainfall forecasts for south-eastern and eastern Australia using climatic indices, Theor. Appl. Climatol. 124 (2016) 1045–1063, https://doi.org/10.1007/s00704-015-1457-3.

[30] N. Nicholls, W. Murray, Workshop on indices and indicators for climate extremes: asheville, NC, USA, 3-6 June 1997 breakout group B: precipitation, Clim. Change 42 (1999) 23–29, https://doi.org/10.1023/A:1005495627778.

[31] A. Yenehun, K. Walraevens, O. Batelaan, Spatial and temporal variability of groundwater recharge in Geba basin, Northern Ethiopia, J. Afr. Earth Sci. 134 (2017) 198–212, https://doi.org/10.1016/j.jafrearsci.2017.06.006.

[32] T. Gebreyohannes, F. De Smedt, K. Walraevens, S. Gebresilassie, A. Hussien, M. Hagos, K. Amare, J. Deckers, K. Gebrehiwot, Application of a spatially distributed water balance model for assessing surface water and groundwater resources in the Geba basin, Tigray, Ethiopia, J. Hydrol. 499 (2013) 110–123, https://doi.org/10.1016/j.jhydrol.2013.06.026.

[33] K. Walraevens, T. Gebreyohannes Tewolde, K. Amare, A. Hussein, G. Berhane, R. Baert, S. Ronsse, S. Kebede, L. Van Hulle, J. Deckers, K. Martens, M. Van Camp, Water balance components for sustainability assessment of groundwater-dependent agriculture: example of the Mendae plain (Tigray, Ethiopia), Land Degrad. Dev. 26 (2015) 725–736, https://doi.org/10.1002/ldr.2377.

[34] K.A. Tekle, I. Yoshida, M. Harada, Nitrate concentration in drinking groundwater wells of Mekelle, Ethiopia, J. Rainwater Catch. Sys. 10 (2004) 1–5, https://doi.org/10.7132/jrcsa.KJ00003257771.

[35] G. Godif, B.R. Manjunatha, Prioritizing sub-watersheds for soil and water conservation via morphometric analysis and the weighted sum approach : a case study of the Geba river basin in Tigray , Ethiopia, Heliyon 8 (2022) e12261, https://doi.org/10.1016/j.heliyon.2022.e12261.

[36] T. Gebreyohannes, F. De Smedt, K. Walraevens, Regional groundwater flow modeling of the Geba basin , northern Ethiopia, Hydrogeological Processes 25 (2017) 639–655, https://doi.org/10.1007/s10040-016-1522-8.

[37] K. Tesfagiorgis, T. Gebreyohannes, F. De Smedt, J. Moeyersons, M. Hagos, J. Nyssen, J. Deckers, Evaluation of groundwater resources in the Geba basin, Ethiopia, Bull. Eng. Geol. Environ. 70 (2010) 461–466, https://doi.org/10.1007/s10064-010-0338-3.

[38] K. Walraevens, I. Vandecasteele, K. Martens, J. Nyssen, J. Moeyersons, T. Gebreyohannes, F. de Smedt, J. Poesen, J. Deckers, M. van Camp, Groundwater recharge and flow in a small mountain catchment in northern Ethiopia, Hydrol. Sci. J. 54 (2009) 739–753, https://doi.org/10.1623/hysj.54.4.739.

[39] FAO, Coping with Water Scarcity: a Strategic Issue and Priority for System-wide Action, Rome, 2006.

[40] N. Alamdari, D.J. Sample, A.C. Ross, Z.M. Easton, A.C. Ross, Evaluating the impact of climate change on water quality and quantity in an urban watershed using an ensemble approach, Estuar. Coast 43 (2020) 56–72, https://doi.org/10.1007/s12237-019-00649-4.

[41] E.C. Brevik, The potential impact of climate change on soil properties and processes and corresponding influence on food security, Agriculture 3 (2013) 398–417, https://doi.org/10.3390/agriculture3030398.

[42] J.S. Bandara, Y. Cai, The impact of climate change on food crop productivity , food prices and food security in South Asia, Econ. Anal. Pol. (2014), https://doi.org/10.1016/j.eap.2014.09.005.

[43] M. Cheng, B. Mccarl, C. Fei, Climate change and livestock production : a literature review, Atmosphere 13 (2022), https://doi.org/10.3390/atmos13010140.

[44] I.R. Lake, L. Hooper, A. Abdelhamid, G. Bentham, A.B.A. Boxall, A. Draper, S. Fairweather-tait, M. Hulme, P.R. Hunter, G. Nichols, K.W. Waldron, Review climate change and food security : health impacts in developed countries, Environ. Health Perspect. 120 (2012) 1520–1526.

[45] R. Affoh, H. Zheng, K. Dangui, B.M. Dissani, The impact of climate variability and change on food security in sub-saharan Africa : perspective from panel data analysis, Sustainability 14 (2022), https://doi.org/10.3390/su14020759.

[46] K.N. Disasa, H. Yan, G. Wang, J. Zhang, C. Zhang, X. Zhu, Projection of future precipitation , air temperature, and solar radiation changes in southeastern China, Theor. Appl. Climatol. (2024) 4481–4506, https://doi.org/10.1007/s00704-024-04891-0.

[47] A.A. Fenta, H. Yasuda, K. Shimizu, N. Haregeweyn, Response of streamflow to climate variability and changes in human activities in the semiarid highlands of northern Ethiopia, Reg. Environ. Change (2017), https://doi.org/10.1007/s10113-017-1103-y.

[48] A.A. Adesete, O.E. Olanubi, R.O. Dauda, Climate change and food security in selected sub - saharan African countries, Environ. Dev. Sustain. 25 (2023), https://doi.org/10.1007/s10668-022-02681-0.

[49] S. Saha, S. Moorthi, H.-L. Pan, X. Wu, J. Wang, S. Nadiga, P. Tripp, R. Kistler, J. Woollen, D. Behringer, H. Liu, D. Stokes, R. Grumbine, G. Gayno, J. Wang, Y.-T. Hou, H.-Y. Chuang, H.-M.H. Juang, J. Sela, M. Iredell, R. Treadon, D. Kleist, P. Van Delst, D. Keyser, J. Derber, M. Ek, J. Meng, H. Wei, R. Yang, S. Lord, H. Van Den Dool, A. Kumar, The NCEP climate Forecast system reanalysis, Amer. Meteorol. Soc. (2010), https://doi.org/10.1175/2010BAMS3001.1.

[50] Z. Duan, Y. Tuo, J. Liu, H. Gao, X. Song, Z. Zhang, L. Yang, D. Mekonnen, Hydrological evaluation of open-access precipitation and air temperature datasets using SWAT in a poorly gauged basin in Ethiopia, J. Hydrol. 569 (2019) 612–626, https://doi.org/10.1016/j.jhydrol.2018.12.026.

[51] E. Kalnay, M. Kanamitsu, R. Kistler, W. Collins, D. Deaven, L. Gandin, M. Iredell, S. Saha, G. White, J. Woollen, Y. Zhu, M. Chelliah, W. Ebisuzaki, W. Higgins, J. Janowiak, K.C. Mo, C. Ropelewski, J. Wang, A. Leetmaa, R. Reynolds, R. Jenne, D. Joseph, The NCEP/NCAR 40-year reanalysis project, Bull. Am. Meteorol. Soc. 77 (1996) 437–472, https://doi.org/10.1175/1520-0477.

[52] R.L. Wilby, C.W. Dawson, Statistical Downscaling Model (SDSM), Version 4.2, A Decision Support Tool for the Assessment of Regional Climate Change Impacts, 2007. United Kingdom.

[53] D.N. Moriasi, M.W. Gitau, N. Pai, P. Daggupati, Hydrologic and water quality models: performance measures and evaluation criteria, Trans. ASABE 58 (2015) 1763–1785, https://doi.org/10.13031/trans.58.10715.

[54] J. Nash, J. Sutcliffe, River flow forecasting through conceptual models part I—a discussion of principles, J. Hydrol. 10 (1970) 282–290, https://doi.org/10.1016/0022-1694(70)90255-6.

[55] D.N. Moriasi, J.G. Arnold, M. Liew, R.L. Bingner, R.D. Harmel, T.L. Veith, Model evaluation guidelines for systematic quantification of accuracy in watershed simulations, Trans. ASABE 50 (2007) 885–900, https://doi.org/10.13031/2013.23153.

[56] F.J. Moral, F.J. Rebollo, L.L. Paniagua, A. García-Martín, F. Honorio, Spatial distribution and comparison of aridity indices in Extremadura, southwestern Spain, Theor. Appl. Climatol. (2015), https://doi.org/10.1007/s00704-015-1615-7.

[57] E. Baltas, Spatial distribution of climatic indices in northern Greece, Meteorol. Appl. 14 (2007) 69–78, https://doi.org/10.1002/met.7.

[58] M. Fazzini, C. Bisci, P. Billi, The climate of Ethiopia, in: P. Billi (Ed.), Landscapes and Landforms of Ethiopia, Springer Science+Business Media, Dordrecht, 2015, p. 389, https://doi.org/10.1007/978-94-017-8026-1.

[59] K. Braganza, D.J. Karoly, J. Arblaster, Diurnal temperature range as an index of global climate change during the twentieth century, Geophys. Res. Lett. 31 (2004), https://doi.org/10.1029/20046L019998.

[60] D.R. Easterling, B. Horton, P.D. Jones, T.C. Peterson, T.R. Karl, D.E. Parker, M.J. Salinger, V. Razuvayev, N. Plummer, P. Jamason, C.K. Folland, Maximum and minimum temperature trends for the globe, Science 277 (1997) 364–367, https://doi.org/10.1126/science.277.5324.364.

[61] L. V Alexander, X. Zhang, T.C. Peterson, J. Caesar, B. Gleason, A.M.G.K. Tank, M. Haylock, D. Collins, B. Trewin, F. Rahimzadeh, A. Tagipour, K.R. Kumar, J. Revadekar, G. Griffiths, L. Vincent, D.B. Stephenson, J. Burn, E. Aguilar, M. Brunet, M. Taylor, M. New, P. Zhai, M. Rusticucci, J.L. Vazquez-Aguirre, Global observed changes in daily climate extremes of temperature and precipitation, J. Geophys. Res. 111 (2006) 1–22, https://doi.org/10.1029/2005JD006290.

[62] J.L. Martín, J. Bethencourt, E. Cuevas-Agulló, Assessment of global warming on the island of Tenerife , Canary Islands (Spain). Trends in minimum , maximum and mean temperatures since 1944, Clim. Change 114 (2012) 343–355, https://doi.org/10.1007/s10584-012-0407-7.

[63] M.A. Gebremedhin, G.H. Kahsay, H.G. Fanta, Assessment of spatial distribution of aridity indices in Raya valley, northern Ethiopia, Appl. Water Sci. 8 (2018) 1–8, https://doi.org/10.1007/s13201-018-0868-6.

[64] A. Ramachandran, D. Praveen, R. Jaganathan, K. Palanivelu, Projected and observed aridity and climate change in the east coast of south India under RCP 4 . 5, Sci. World J. 2015 (2015), https://doi.org/10.1155/2015/169761.

[65] S. Bahmani, H. Salimi, H. Sanikhani, Spatiotemporal analysis of aridity indices by using the nonparametric methods (case study: sirvan river basin, Kurdistan Province, Iran), Arabian J. Geosci. 14 (2021), https://doi.org/10.1007/s12517-021-07813-w.

[66] M. Jafarpour, A. Adib, M. Lotfirad, Ö. Kisi, Spatial evaluation of climate change - induced drought characteristics in different climates based on De Martonne Aridity Index in Iran, Appl. Water Sci. 13 (2023) 1–20, https://doi.org/10.1007/s13201-023-01939-w.

[67] M.A.A. Zarch, B. Sivakumar, H. Malekinezhad, A. Sharma, Future aridity under conditions of global climate change, J. Hydrol. 554 (2017) 451–469, https://doi.org/10.1016/j.jhydrol.2017.08.043.